

The author(s) shown below used Federal funds provided by the U.S. Department of Justice and prepared the following final report:

Document Title: Latent Print Detection by MacroRaman Imaging

Author: R.M. Connatser, Giorgia DePaoli, Charles Gardner, Linda Lewis

Document No.: 230163

Date Received: April 2010

Award Number: 2005-DD-R-094

This report has not been published by the U.S. Department of Justice. To provide better customer service, NCJRS has made this Federally-funded grant final report available electronically in addition to traditional paper copies.

Opinions or points of view expressed are those of the author(s) and do not necessarily reflect the official position or policies of the U.S. Department of Justice.

Report Title: Latent Print Detection by MacroRaman Imaging

Award Number: 2005-DD-R-094

Author(s): R.M. Connatser, Giorgia DePaoli, Charles Gardner, Linda Lewis*
***Principal Investigator**

Team Members:

Linda A. Lewis (PI)

R. Maggie Connatser

Samuel A. Lewis

Giorgia DePaoli

Ellyn Schuette

Oak Ridge National Laboratory

Charles S. Gardner

Rebecca Schuler

Patrick J. Treado

ChemImage Corporation

Abstract

The purpose of this work was to exploit enhanced vibrational spectroscopy to detect latent fingerprints. Supporting studies included using gas and liquid chromatography coupled to mass spectrometry to identify the most promising and resilient chemical constituents of latent prints in order for enhancing spectroscopy to target the most statistically probable remains in a fingerprint. This would, therefore, significantly increase the likelihood that any print, but particularly those exposed to thermal events or light damage, would be detected. Exposure to light or heat, or simply a dearth of fingerprint material, renders some latent fingerprints undetectable using conventional methods. We begin to address such elusive fingerprints using detection targeting photo- and thermally stable fingerprint constituents: surface enhanced Raman spectroscopy (SERS). SERS can give descriptive vibrational spectra of amino acids, among other robust fingerprint constituents, and good sensitivity can be attained by improving metal-dielectric nanoparticle substrates. Many types of such substrates, both existing in the current literature as well as novel to this project, were explored in pursuit of sufficient vibrational signal sensitivity to detect a latent fingerprint based on its inherent chemical makeup and in difficult conditions. With SERS chemical imaging, vibrational bands' intensities recreate a visual of fingerprint topography. The impact of nanoparticle synthesis route, dispersal methodology – deposition solvent, and laser wavelength are discussed, as are data from enhanced vibrational spectra of fingerprint components. SERS and Raman chemical images of fingerprints and realistic contaminants are shown. To our knowledge, this represents the first SERS imaging of fingerprints. In conclusion, this work progresses toward the ultimate goal of vibrationally detecting latent prints that would otherwise remain undetected using traditional development methods. Photo- and thermal-degradation studies on eccrine fingerprint components are also presented herein. These studies were undertaken in order to focus detection strategies with SERS reagents to the most survivable of all the fingerprint constituents. Dilute, distinct solutions of urea, lactic acid and seven amino acids were deposited on steel coupons and Teflon® disks, exposed to artificial sunlight or heat, extracted, and analyzed. This study's aim was to determine whether the investigated eccrine components, previously determined to be generally Raman

active in our initial survey of all components, experienced photo – or thermally induced degradation, and if so, to determine the rate and identify any detectable products. Neither the amino acids nor urea exhibited photo-degradation; however, when heated for a period of three minutes, the onset of thermal degradation was initiated at 100°C for the amino acids and 100°C for urea. Lactic acid, the major polymerization initiator of superglue fuming, showed both photochemical and thermal degradation. These results could be used for future development of new latent fingerprint visualization methods, especially when lactic acid is degraded. Although the enhancement factor of SERS substrates is as yet insufficient to facilitate the detection of the most difficult prints, the conclusions reached about the feasibility of SERS fingerprint detection and especially thermal and photo-degradation of prints include useful information for improving all methods of latent detection, both traditional and novel. The ultimate success of this technique will come with the creation of a SERS enhancing reagent that offers, and retains upon dispersal to a remote surface, the 1×10^7 magnitude signal enhancement purported by tailor-made, in situ advanced substrates being tested with strong Raman responders, as opposed to weaker Raman responders such as amino and fatty acids.

Table of Contents

	Section	Page #
1.	Abstract	1
2.	Executive Summary	4
3.	Main Report Section I: Introduction	14
4.	Main Report Section II: Methods	17
5.	Main Report Section III: Results and Discussion of Findings	26
6.	Main Report Section IV: Conclusions	30
7.	Main Report Section V: References	31
8.	Main Report Section VI: Dissemination of Research Findings	34

Executive Summary

I. Problem and Purpose

Fingerprint evidence offers great value to criminal investigations; it is no surprise, then, that enhancement of fingerprint development technologies remains an active area of research within the forensic science community. Over the years, great diversity in latent fingerprint development techniques has unfolded for use with the various print types and surface matrices that are encountered. Yet, despite the many advances, situations still remain in which print development is inconsistent or completely unsuccessful. One such situation involves the exposure of deposited prints to high temperatures, such as those created by a detonation, fired ammunition, or evidence from an arson site. There is evidence for thermal decomposition of fingerprint constituents (1, 2), but a thorough characterization of the decomposition processes and products is lacking. Another problematic situation involves the aging of prints in the presence of light. Recent work in our group identified sodium lactate as the major initiator of the cyanoacrylate polymerization that occurs during the popular superglue fuming technique, and then went on to describe the degradation (and subsequent failure of print development) that resulted when the lactate in a fingerprint deposit was exposed to light (3). How many other instances of a print development method performing poorly as prints age could be the result of the thermal or photo-degradation of the key reactant within the fingerprint deposit? Wouldn't a development strategy that could sensitively detect persistent intrinsic fingerprint constituents be an advantage to detecting such degraded fingerprints? Addressing these questions was the purpose of the work described herein. The identification of this two-fold challenge underscored the need for a thorough study of possible light and/or heat degradation of other fingerprint components coupled with the development of an enhanced Raman technique to selectively image a fingerprint based on the chemical signature of its intrinsic residual constituents. Once such thermal and photodegradation information is available, the forensic research community would be in a much better position to develop robust new fingerprint visualization techniques by targeting the stable components, as well as their degradation products. Thus, this project approached the problem from two directions, first by characterizing the photo- and thermal degradation of fingerprint materials that individually exhibited any promise of surface enhanced Raman scatter (SERS) and second by developing a novel use of Raman scatter, a vibrational spectroscopy, enhanced with metal nanoparticles to create a sensitive imaging approach for degraded fingerprints.

Latent eccrine fingerprints deposited on many surfaces may sometimes go undetected once prints age over a few hours, especially when exposed to sunlight. The ability to develop latent fingerprints is often influenced by many factors including print-type (clean/eccrine through oily/sebaceous), humidity, light, surface matrix, etc.(4) Recent findings on the fundamental chemistry of superglue fuming, a prominent method for developing prints on non-porous surfaces, revealed methods capable of enhancing the ability to develop latent fingerprints that would otherwise go undetected.(5) This enhancement, which involves fuming with acetic acid vapors prior to superglue fuming, was not highly effective on fingerprints exposed to high energy (UV/blue light) radiation from sun or fluorescent lighting, especially on surfaces containing iron (III), due to the catalyzed photodegradation of lactate anion, which is the major cyanoacrylate polymerization initiator.(6) In addition, the acetic acid enhancement method is not easily amenable to field applications. Thus, a real need exists to detect latent fingerprints on all surfaces regardless of the print type or environmental exposure factors. This work on latent print

detection will lead to a better understanding of fingerprint degradation chemistry. It will also facilitate a new, complementary method for Raman-based latent print visualization by utilizing the surface enhancement phenomenon to achieve sensitive chemical imaging-based latent print detection for field applications.

II. Research Design

Our research began with the identification of a surrogate fingerprint solution we could use to age and test our methods at increased concentrations without the hindrance of constantly relying on the lab members' ability to lay down 5, 10, or even 200 clean eccrine fingerprints on each sample. A deposited fingerprint can be classified as one of two general print types based on composition: an eccrine (clean) print, or a sebaceous (oily) print. Eccrine prints contain only those materials secreted by the eccrine glands, which are found over the entire surface of the skin and in especially high concentrations on the palms of the hands and the soles of the feet (collectively known as the volar surfaces). More than 98% water, the balance of eccrine print composition includes urea, sodium lactate, inorganic salts, free amino acids, free organic acids, and some mucin-like glycoproteins (7, 8, 9). Sebaceous prints include both eccrine secretions and the sebum produced by the sebaceous glands, an oily secretion comprised of free fatty acids, wax esters, squalene, cholesterol esters, and cholesterol (7, 8). The volar surfaces do not contain sebaceous glands, which are located by hair follicles. However, sebaceous prints are prevalent due to the contamination of the fingertips by touching other areas of the body. Regardless of print type, the residue comprising a fingerprint deposit is a complex mixture of compounds. One study alone identified over 300 unique components in a sebaceous print (10). To foster a more manageable study, the scope of the degradation experiments was limited to eccrine fingerprint, which contains the major initiators responsible for superglue polymerization. Whereas a great deal of research has been done on sebaceous secretions (8, 11, 12), there are substantially fewer publications concerning eccrine secretions. This data pool shrinks still further when focusing on quantitation. Our research targeted eccrine prints due to the fact that when exposed to environmental conditions, they quickly become undetectable with conventional technique, in addition to the fact that eccrine constituents are common to clean and oily prints. To create an artificial eccrine fingerprint solution, the authors relied on a study of amino acids in an eccrine thumbprint (13), supplemented by the eccrine sweat entry in the Geigy Scientific Tables (9). Specifically, Raman active eccrine components were targeted based on a preliminary Raman screen done prior to this degradation study. The decision to study eccrine materials was made not only to simplify the composition of the artificial fingerprint solution, but also because eccrine prints are better models of children's fingerprints (14). Children do not begin to secrete sebum until they are between seven and ten years old (7), the usual age range in which adrenal androgens are first produced. Therefore, lessons learned in the study of eccrine print degradation could be applied to the development of fingerprints of both adults and children.

Eccrine components were screened in early trials for Ag-based SERS activity utilizing both nanocomposite substrates and nebulized Ag colloid reagents in order to exploit surface enhancement effects in Raman. The nanocomposite material consists of a polydimethylsiloxane (PDMS) elastomer with 50-100-nanometer diameter silver particles embedded in a three dimensional arrangement in the topmost 250nm of the substrate's surface. For Ag-colloid screening, colloids ranging between 60 – 100 nm were targeted. Of the pure components assayed with Ag-based SERS materials, the following compounds yielded interesting spectra: **urocanic acid, pyruvic acid, orinithine, lactic acid, glycine, urea, threonine, serine, aspartic acid,**

glutamic acid. A significant amount of work was focused on the identification of fingerprint components using gold SERS substrates. A synopsis of the extensive component screening using both silver and gold substrates is provided in **Table 1**, along with a tentative structural assignment for the most prominent vibrational band in each component's spectrum. One particularly encouraging aspect of these studies has been the fact that a vibrational band at $\sim 1100\text{ cm}^{-1}$ is common to urea, a prominent component of eccrine prints, as well as the short chain fatty acid components of both eccrine and sebaceous prints, such as propionic acid and n-hexanoic acid. Since one of the goals of this research is to provide a more universal imaging/development technique for all prints, this common vibrational band could be monitored regardless of print type. Such a find buttresses the basis for latent print detection using macro-Raman imaging.

Table 1: Results of SERS screening of individual fingerprint components at 0.1 mM in water using silver and gold nanocomposite substrates and 633nm or 785 nm wavelength illumination lasers, respectively. Results in italics were only attainable using silver with a 633nm laser. (15, 16)

Fingerprint	SERS Vibrational Bands (cm⁻¹)	Likely Structural Assignment²
Leucine	451-678, ~1450	Amine
Glucose	1223-1416, 1472-1667, 2078-	Carbonyl
Glutamic acid	1577-1612	Carboxylic acid, amine
Histidine	550, 1481-1542, 1577-1612	Amine, amide, carboxylic acid
Threonine	450-720	Amine
Ornithine	1407-1469, 1504-1551	Carbonyl
Urocanic acid	~1250, 1308-1374, 1608-1673	Carboxylic acid, amine, vinyl
Creatinine	550, 1229-1632	Amine
Tyrosine	875, 1445-1598	<i>Benzene ring stretching</i> , Amine
Uric acid	1427-1664	Carboxylic acid, amine
Urea	451-769, 1100	Carboxylic acid, amine (double)
Propionic acid	800, 2275	Hydrocarbon, carboxylic acid
Isovaleric acid	1100	Hydrocarbon, carboxylic acid
n-hexanoic acid	800, 900, 1200, 1375, 1625	Hydrocarbon, carboxylic acid
Isobutyric acid	800, 1100	Hydrocarbon, carboxylic acid
Acetic acid	800, 1100	Hydrocarbon, carboxylic acid
n-butyric acid	800, 1100	Hydrocarbon, carboxylic acid
<i>Aspartic acid</i>	<i>~1475-1580</i>	<i>Carboxylic acid</i>
<i>Serine</i>	<i>550</i>	<i>Amine</i>
<i>Pyruvic acid</i>	<i>~1475-1580</i>	<i>Carboxylic acid</i>
<i>Lactic acid</i>	<i>~1475-1580</i>	<i>Carboxylic acid</i>
<i>Isoleucine</i>	<i>451-575, 1450</i>	<i>Amine</i>
<i>Glycine</i>	<i>1670</i>	<i>Amide</i>

The goal of our gas chromatography- and liquid chromatography-mass spectrometry (GC- and LC-MS) studies was to determine whether any of the tested amino acids experienced photo-induced degradation, and if so, to determine the rate of degradation and identify any detectable degradation products. For amino acids, this was accomplished by monitoring the relative ratio of the peak area of each amino acid to the peak area of the closest-eluting internal standard. Data processing used Bruker Daltonics software (Billerica, MA), and consisted of choosing the extracted ion chromatograms for the amino acid/internal standard, subtracting the baseline, applying 3-cycle smoothing of the chromatogram, and manually integrating the peak area. The literature accompanying the derivatization kit provided the m/z values to monitor for the amino acids and internal standards, as well as the instructions to use the first internal standard (homoarginine, HARG) for comparison with SER, GLY, and THR and the second internal standard (methionine- d_3 , Met- d_3) for comparison with ORN, ASP, HIS, and GLU. For each of the seven amino acids, the relative ratio of the amino acid peak area to the internal standard peak area remained constant across the seven timepoints within the sample set. No notable photo-degradation of the amino acids studied was observed on either Teflon or stainless steel surfaces.

Photo-degradation studies of urea and lactic acid, the choice of extraction solvent (a formic acid-containing water:methanol mix) for the urea and lactic acid samples was compatible with direct infusion into the MS via an atmospheric pressure chemical ionization (APCI) source. Therefore, the collected data consists of spectra; but as with the amino acid, samples, peak area ratios are employed to monitor degradation. The urea samples were analyzed in positive ion mode, with urea producing an M^+ ion at m/z 61, and the melamine used as an internal standard producing an M^+ ion at m/z 127. The lactic acid samples were analyzed in negative ion mode, with lactic acid producing an M^+ ion at m/z 89, and the cyanuric acid used as an internal standard producing an M^+ ion at m/z 128. Two sets of lactic acid and urea samples were exposed to the Xe/HgXe arc lamp for intervals simulating the following periods of time: 0, 2, 5, 7, 14, 28, and 56 days. Each sample was then injected twice for 24 seconds. This approach provided sufficient data to yield statistically meaningful qualitative information about the physical and chemical characteristics of the analytes. As in the amino acids experiments, the aim of these studies was to determine urea and lactic acid photo-induced degradation, the rate of degradation, and identify any degradation products. For each set of samples, the amount of lactic acid and urea recovered on Teflon® discs and steel coupons was calculated. For pyruvic acid, the ingrowth was calculated only as its relative ratio (on Teflon® discs and steel coupons) to the internal standard peak area, since it was a degradation product. Results showed that urea exposed to light did not appear to undergo degradation, even for long exposure times. This set of experiments sought to confirm what is well known, urea does not undergo photodegradation. A different result, however, arose for lactic acid samples exposed to light. The ingrowth of pyruvic acid was found to correlate with lactic acid photo-degradation. Light, catalyzed by the presence of iron ions, seems to play a fundamental role in the production of pyruvic acid as the degradation product. According to our results, after only two days' equivalent of light exposure, the amount of lactic acid was reduced prominently from the initial concentration deposited. Comparing the slope of the curves, decay on steel is faster than on Teflon®. With its high iron content, the steel itself is involved in the lactic acid degradation process, along with the light. The result of this cooperation would be an increase in the speed of the degradation reaction. On the contrary, Teflon®, would act only as an inert platform for the experiments. After monitoring the pyruvic acid peak, it was observed that, along with the lactic acid decomposition, the pyruvic acid also degrades under exposure to light as well as air. However, correlating the rate of

degradation of pyruvic acid to lactic acid we noticed an inflection point around the 28th day of equivalent light exposure, indicating that something was inhibiting the rate of lactic acid degradation. The fact that the rate of degradation did not follow the same rate confirmed that many factors, both chemical and physical, were involved in the degradation process. We speculate that the rate could be influenced by a threshold amount of degraded lactic acid necessary to produce a detectable amount of pyruvic acid. In order to reach this amount, another parameter should be considered: the time required by the light to reach and degrade layers of lactic acid underneath the outer layer. This period of time could be around 4 weeks. Another interesting result is the slightly earlier in-growth of pyruvic acid on the Teflon® relative to steel. This difference may indicate an interaction between the lactate and components of the steel, which temporarily delays conversion to pyruvic acid relative to the inert Teflon®, where the light acts alone to convert lactic to pyruvic.

For thermal degradation studies of amino acids, all seven amino acids deposited on steel were degraded to some extent in the presence of heat. Serine and glycine data yielded a large-scale reduction in detected amino acid for the sample heated to 150°C, and no peak was present for threonine at that temperature. Ornithine, aspartic acid, histidine, and glutamic acid all experienced a similar degradation pattern: there was substantial amino acid loss incurred at the 100°C temperature point, and additional loss at the 150°C sample. Unfortunately, when the chromatograms were analyzed for in-growth products, none could be found. For thermal degradation studies of urea and lactic acid, two sets of samples of lactic acid and urea on steel were analyzed at different temperatures: room temperature, 50°C, 100°C and 150°C. Each sample was then injected twice for 24 seconds. For the samples containing lactic acid, the M⁺ peak of pyruvic acid at m/z 87 was also monitored. For each set of samples, the amount of lactic acid and urea recovered, and the relative ratio of pyruvic acid to the internal standard peak area on steel coupons was calculated. Already an object of studies (17), our results confirmed the fact that urea's thermal decomposition was initiated around 150°C. In contrast, the lactic acid thermal degradation process started between 50 and 100°C along with pyruvic acid generation and subsequent degradation.

III. Findings/Conclusions/Implications for Policy and Practice

Building from success with individual component SERS screening of fingerprint constituents using silver colloid and silver nanocomposite, which is not fieldable due to its solid nature (it cannot be dispersed onto remote surfaces), we investigated other more recently developed SERS substrates. The relatively nontoxic nature of metal colloids in their SERS format and the portability of Raman spectrometers and imaging units all point toward high feasibility of a fully fieldable method. Hence, an investigation was initiated into the application of SERS imaging to detecting difficult prints, even on porous surfaces due to the depth of focus and other physical micro-properties including wettability, hydrophobicity, and curvature. The experiments in this work proved the concept of SERS fingerprint imaging and laid the groundwork (Figures 1, 3, 4; Table 1) for an emerging technology with the potential capacity to discern otherwise irretrievable prints and many classes of information-rich print contaminants, such as drugs or explosives, all based on their inherent chemical vibrational signal and the intense possibility of enhanced Raman scatter (1×10^7 increases in Raman signals for surface enhancement are have been shown by multiple groups).(18-20) This potential must be fully tested against traditional methods as improved SERS substrates are developed, although anecdotal comparisons have been promising thus far. On the heat and light exposed, porous, and

overall low total material content prints targeted, we do not observe the darkened print image optically resulting from Physical Developer solutions from the fingerprint treated with SERS enhancement reagent, even when examined under a RUVIS. The applicability of SERS imaging for widespread fingerprint detection relies on dispersed SERS reagents offering 1×10^7 scatter signals quoted in the academic SERS literature for non-dispersed reagents. Finally, Figure 1 also helps illustrate the feasibility of this technique, as it shows a surface enhanced Raman response of 5x concentrated eccrine fingerprint material that has been deposited on polyvinyl chloride tubing filled with a low explosive and subsequently ignited. The fingerprint solution and SERS reagent nanowires were deposited, dried, and the scattering measured after the model miniature ignition event. The response shown demonstrates that bands representative of such relevant background interferents as explosives are discernible from fingerprint spectral responses. Evidentiary information beyond collection of the latent fingerprint image could be gleaned from the careful characterization of these interferent spectra, as well as spectra from other potential fingerprint contaminants such as drugs of abuse, bioterror agents or residues, or high explosives. The practicality and reliability of a dual-duty application of SERS imaging for fingerprints and

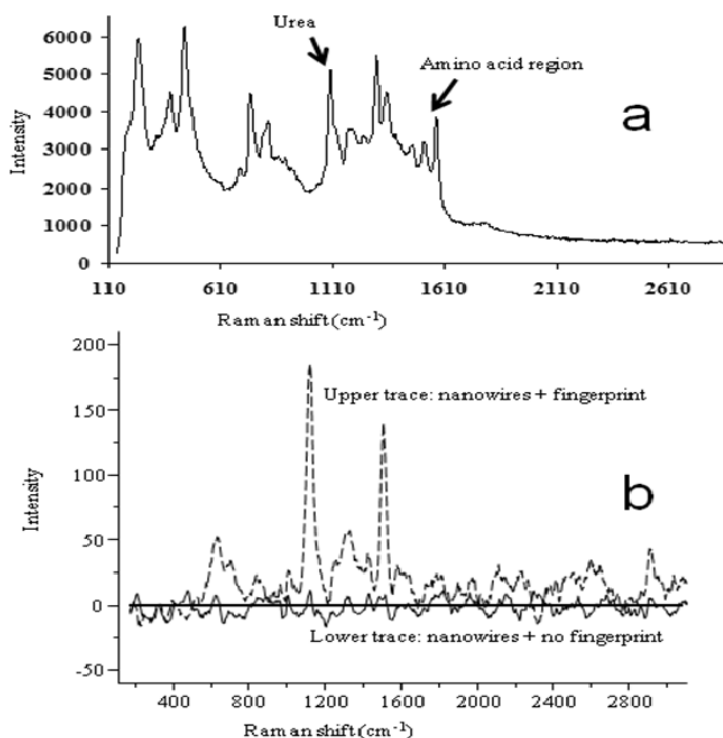


Figure 1: Comparison of simple colloid and advanced SERS nanoparticles. (a) Spectrum from eccrine print material detected at realistic concentration with conventional silver colloid. *Note that a significant background is present from the silver reducing citrate solution. (b) Spectrum of 5x concentrated eccrine material on porous steel with nanowires from NRL. *Note much lower background and less overall signal.

their contaminants is being explored further as our group continues to develop the SERS macro-Raman imaging technique. The success of SERS chemical imaging of latent fingerprints relies heavily upon the creation of a high enhancement factor SERS metal nanoparticle substrate that retains its field-amplifying characteristics upon dispersal. The synthesis and testing of just such an improved SERS reagent will be founded upon the preliminary studies related here, and this is the current occupation of our research efforts. Once more adequate SERS reagent sensitivity is achieved, comparison studies to gauge this new niche technique's overall utility versus established methods will be executed and reported. The use of SERS imaging of fingerprints and fingerprint degradation products, will become a useful ancillary tool for imaging prints that other techniques cannot bring out due to a lack of the right materials (a lack of the lactate anion, for instance, in the case of super glue fuming). Beyond scientific analytical validation, policies for

when and where to use SERS imaging for latent prints will have to be developed based on the needs of the technical practitioners as well as field law enforcement agents.

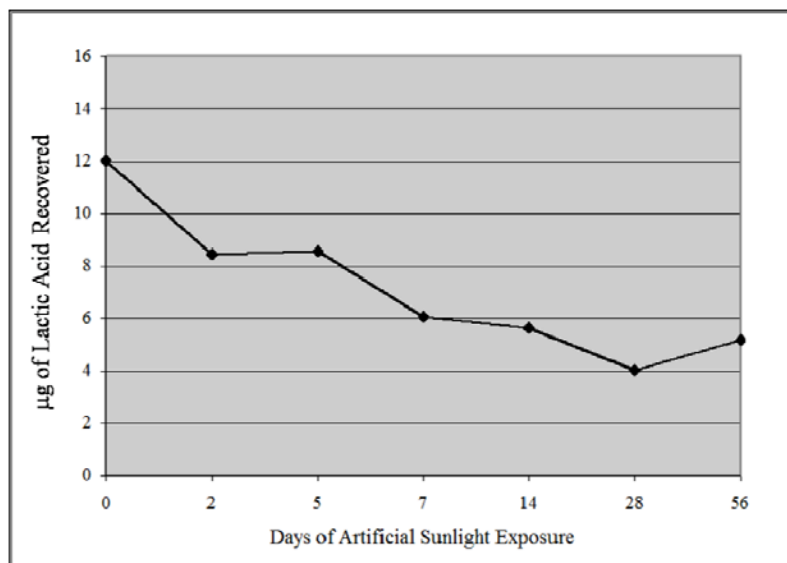


Figure 2: Reduction of lactic acid from fingerprint test residues under exposure to sunlight simulator.

APCI mass spectrometry of urea and HPLC of amino acids showed that these components were not affected by the action of light (even for long equivalent times of exposure) or interaction with different types of material. In contrast, photo-degradation experiments on lactic acid indicated a significant reduction of the initial concentration of the acid itself after just two days' equivalent of light exposure, with a concomitant degradation of its ingrowth product, pyruvic acid. Lactic acid's degradation is charted in Figure 2. However, for lactic acid samples on steel and

Teflon, the degradation rate of pyruvic acid ingrowths to the lactic acid present, slowed down around the 28th day of light exposure. Analysis of amino acids exposed to heat established the temperature tolerated prior to the complete decomposition process for this class of components. All seven amino acids deposited on Teflon® disks and steel coupons exposed to 150°C were undetectable in the analysis with HPLC. However, no degradation product was found. Similar results were obtained for urea, indicating the onset of degradation at 150°C. Lactic acid and its photo-degradation product pyruvic acid are both affected by heat exposure. The beginning of their decomposition process was marked at 50°C.

Preliminary studies of the Raman response of sebaceous fingerprints were carried out on a SERS active nanocomposite silver substrate and on a non-SERS active aluminum substrate. The substrate was removed from the vacuum, a sebaceous fingerprint deposited on the slide and analyzed on the ChemImage FALCON II system with 532 nm laser excitation. **Figure 3** shows the imaging of fingerprint ridges using the enhanced Raman response induced by the silver surface. In these images, the C-H bonds present in the fingerprint oil generate the Raman signal. Each of the images is a montage of smaller fields of view, stitched together to show a larger image, better suited for identification purposes. Figure 3 also includes a comparison of the Raman spectra for the substrate, a fingerprint on the SERS active substrate, and a fingerprint oil spectrum collected on a non-SERS active substrate. In order to better evaluate the Raman response improvement resulting from the SERS active substrate, a set of Raman images was collected from a sebaceous fingerprint on a mirrored aluminum surface, which is known to be non-SERS active. This data is shown in Figure 4.

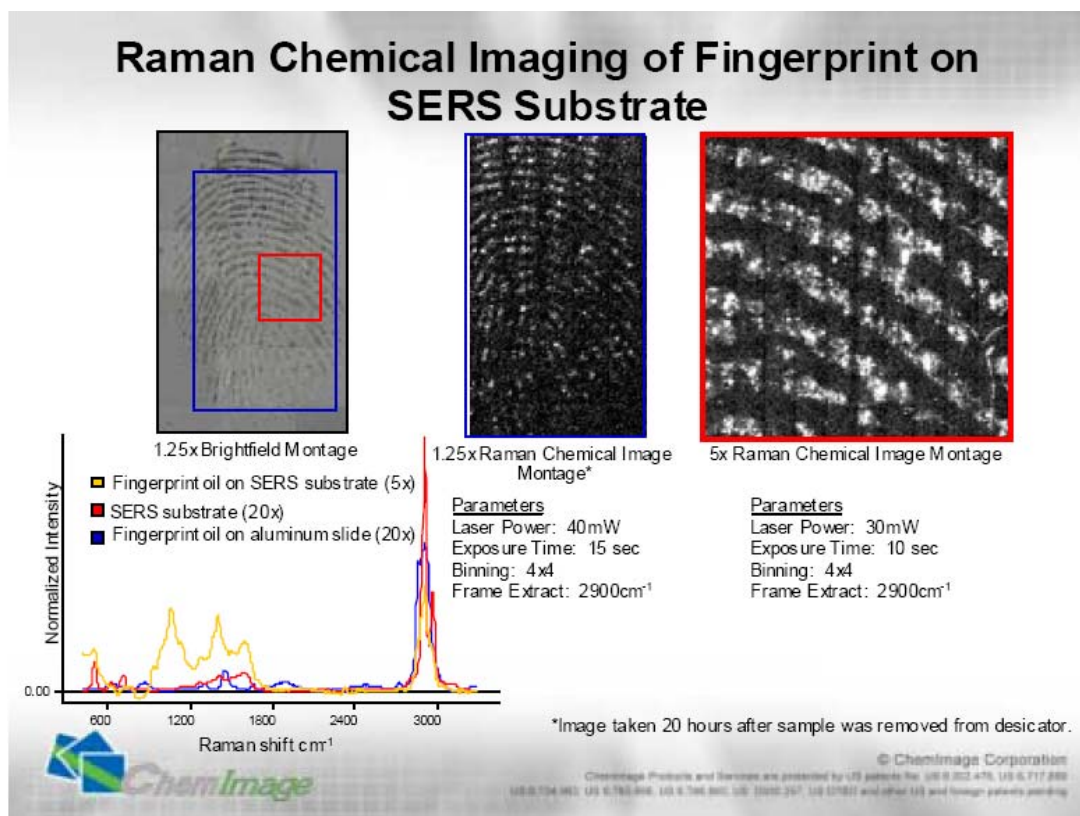


Figure 3. Raman imaging of a sebaceous fingerprint on a silver nanocomposite substrate

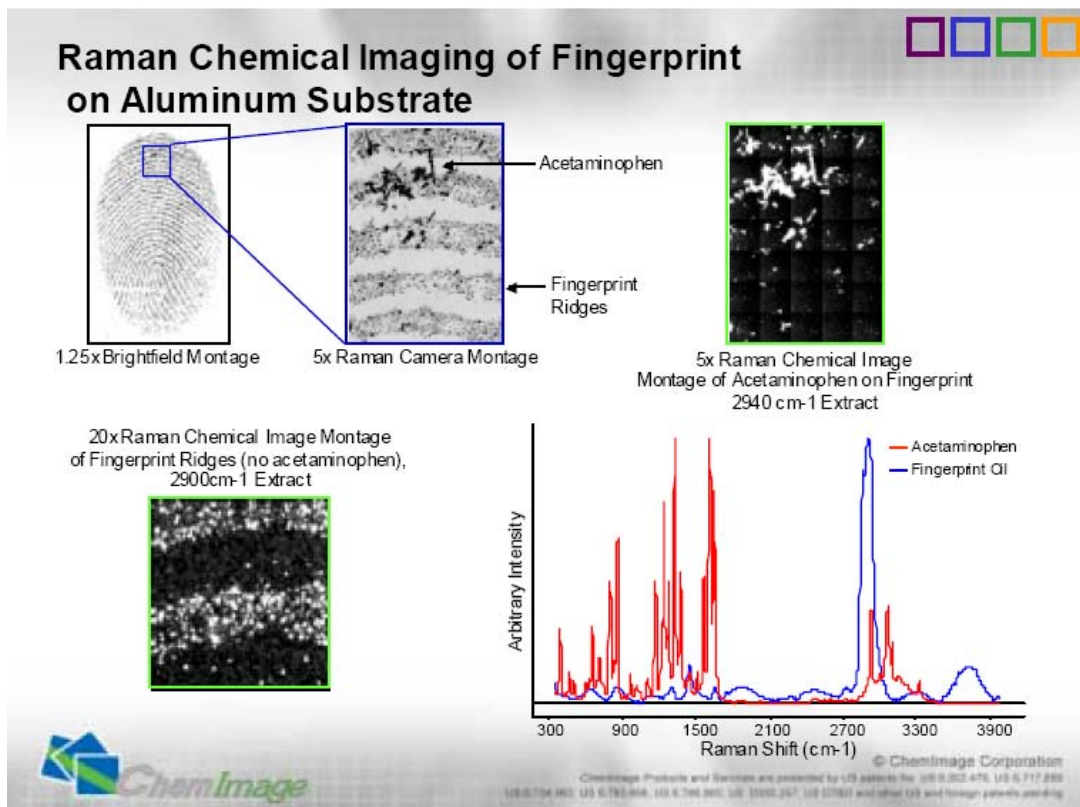


Figure 4. Raman imaging of a sebaceous fingerprint on an aluminum substrate

While it is not directly evident in these images, the hydrocarbon region Raman response was much lower compared with the nanocomposite silver surface. Additionally, these experiments were designed to show the feasibility of Raman imaging to detect drugs of abuse (DOA) particles co-located with a fingerprint. Here acetaminophen (active ingredient in Tylenol®) was used as a DOA simulant and is easily imaged within the ridges of the fingerprint. These preliminary experiments clearly demonstrated the proof of concept for SERS-based Raman imaging of fingerprints. These experiments also provide the first response data for use in validating the mathematical models used to govern the design of a Transportable Raman Fingerprint Imaging System.

Results achieved in this work are expected to be useful to the future development of fingerprint visualization methods. Specifically, the target of these methods would be latent fingerprints arisen from typical scenarios where the application of the superglue fuming technique could be fallible due to the degradation of the components that initiate polymerization.

NIJ Final Report Main Body
Award No. 2005-DD-R-094: Latent Print Detection by MacroRaman Imaging

I. Introduction

Statement of the problem:

Latent eccrine fingerprints deposited on many surfaces may sometimes go undetected once prints age over a few hours, especially when exposed to sunlight. The ability to develop latent fingerprints is often influenced by many factors including print-type (clean/eccrine through oily/sebaceous), humidity, light, surface matrix, etc.(4) Recent findings on the fundamental chemistry of superglue fuming, a prominent method for developing prints on non-porous surfaces, revealed methods capable of enhancing the ability to develop latent fingerprints that would otherwise go undetected.(5) This enhancement, which involves fuming with acetic acid vapors prior to superglue fuming, was not highly effective on fingerprints exposed to high energy (UV/blue light) radiation from sun or fluorescent lighting, especially on surfaces containing iron (III) due to the catalyzed photodegradation of a lactate anion, which is the major cyanoacrylate polymerization initiator.(6) In addition, the acetic acid enhancement method is not easily amenable to field applications. Thus, a real need exists to detect latent fingerprints on all surfaces regardless of the print type or environmental exposure factors. This work on latent print detection will lead to a better understanding of fingerprint degradation chemistry. It will also facilitate a new, complementary method for Raman-based latent print visualization by utilizing the surface enhancement phenomenon to achieve sensitive chemical imaging-based latent print detection for field applications. To accomplish this goal, the project was divided into two phases. The objective of the first part was to study the fingerprint chemistry and decomposition with respect to Raman detection and enhancement methods with an aim to eventually validate the concept of a transportable macro-Raman system. The second part, a fully fieldable imaging system, relied on the development of a dispersible SERS reagent system of intense inherent sensitivity currently being researched in our labs. These tasks are in support of a National Institute of Justice (NIJ) funded program to develop improved visualization techniques for latent fingerprints.

Literature citations and review

Fingerprint evidence offers great value to criminal investigations; it is no surprise, then, that fingerprint development remains an active area of research within the forensic science community. Over the years, great diversity in latent fingerprint development techniques has unfolded for use with the various print types and surface matrices that are encountered. Yet, despite the many advances, situations still remain in which print development is inconsistent or completely unsuccessful. One such situation involves the exposure of deposited prints to high temperatures, such as those created by an IED detonation, fired ammunition, or evidence from an arson site. There is evidence for thermal decomposition of fingerprint constituents (1, 2), but a thorough characterization of the decomposition processes and products is lacking. Another problematic situation involves the aging of prints in the presence of light. Recent work by Lewis identified sodium lactate as the major initiator of the cyanoacrylate polymerization that occurs during the popular superglue fuming technique, and then went on to describe the degradation (and subsequent failure of print development) that resulted when the lactate in a fingerprint deposit was exposed to light (3). How many other instances of a print development method

performing poorly as prints age could be the result of the thermal or photo-degradation of the key reactant within the fingerprint deposit? This discovery underscores the need for a thorough study of possible light and/or heat degradation of other fingerprint components. Once such thermal and photodegradation information is available, scientists would be in a much better position to develop successful fingerprint visualization techniques by targeting the stable and degradation products. Thus, the current study was embarked upon to provide that characterization of photo- and thermal degradation of fingerprint materials.

A deposited fingerprint can be classified as one of two general print types based on composition: an eccrine (clean) print, or a sebaceous (oily) print. Eccrine prints contain only those materials secreted by the eccrine glands, which are found over the entire surface of the skin and in especially high concentrations on the palms of the hands and the soles of the feet (collectively known as the volar surfaces). More than 98% water, the balance of eccrine print composition includes urea, sodium lactate, inorganic salts, free amino acids, free organic acids, and some mucin-like glycoproteins (7, 8, 9). Sebaceous prints include both eccrine secretions and the sebum produced by the sebaceous glands, an oily secretion comprised of free fatty acids, wax esters, squalene, cholesterol esters, and cholesterol (7, 8). The volar surfaces do not contain sebaceous glands, which are located by hair follicles. However, sebaceous prints are prevalent due to the contamination of the fingertips by touching other areas of the body. Regardless of print type, the residue comprising a fingerprint deposit is a complex mixture of compounds. One study alone identified over 300 unique components in a sebaceous print (10). To foster a more manageable study, the scope of the degradation experiments was limited to eccrine fingerprint, which contains the major initiators responsible for superglue polymerization. Whereas a great deal of research has been done on sebaceous secretions (8, 11, 12), there are substantially fewer publications concerning eccrine secretions. This data pool shrinks still further when focusing on quantitation. Our research targeted eccrine prints due to the fact that when exposed to environmental conditions, they quickly become undetectable with conventional technique, in addition to the fact that eccrine constituents are common to clean and oily prints. To create an artificial eccrine fingerprint solution, the authors relied on a study of amino acids in an eccrine thumbprint (13), supplemented by the eccrine sweat entry in the Geigy Scientific Tables (9). Specifically, Raman active eccrine components were targeted in support of a Raman imaging technique being developed at ORNL in parallel with this degradation study.

The decision to study eccrine materials was made not only to simplify the composition of the artificial fingerprint solution, but also because eccrine prints are better models of children's fingerprints (14). Children do not begin to secrete sebum until they are between seven and ten years old (7), the usual age range in which adrenal androgens are first produced. Therefore, lessons learned in the study of eccrine print degradation could be applied to the development of fingerprints of both adults and children.

Raman spectroscopy is executed when the inelastically scattered photons from a molecule are collected and their energy differences translated into a wavenumber spectrum indicative of the vibrating bonds within the molecule.(19) Surface enhancement results when an analyte molecule's proximity with a metal surface allows the amplification of two electromagnetic fields: the one impinging on the molecule and the one scattered by the molecule.(20,21) Additionally chemical enhancement may be achieved between analyte and metal through the quenching of fluorescence, a significant source of non-descript background in Raman.(18) However, chemical interactions are also detrimental in some cases due to the repulsion between molecule and metal surface and steric obstruction of the metal surface by non-

analyte ambient molecules. The role of Raman spectroscopy as a forensic tool has already been well established in terms of drug identification, document and currency verification, and, most prominently, art and archaeology verification and dating.(22-26) SERS of amino acids has found broad application in the study of protein folding investigations and simply in detecting certain proteins in an aqueous environment.(27) Urea and lactic acid separately have also been evaluated using Raman as specific markers of physiological imbalance in diabetes and muscle conditions, respectively.(13,14) Raman detection was even pioneered in fingerprint and contaminant detection on a spot detection basis in 2004.(17) Despite these prior uses of Raman spectroscopy for non-imaging fingerprint forensics and the Raman detection of prominent components of eccrine prints in biomedicine, no confluence of these streams of research has yet occurred to produce Raman chemical imaging detection of latent fingerprints. In the research described herein, preliminary groundwork toward developing a technique aimed to use surface enhanced Raman imaging of latent fingerprints is presented.

The science of retrieving latent fingerprints or their images has been well established and continues to improve as new technologies arise in the fundamental fields of science, such as physics, chemistry, and biology. The last two decades have seen the forensic field begin to reap more direct and immediate benefits from advances in fundamental biochemical and analytical chemical research. A few examples of these new technologies include advanced fluorescent tagging, DNA mapping and matching, and the use of data mining techniques in combination with extensive fingerprint databases to electronically catalog latent prints and comparatively identify them. (31-33) Vibrational spectroscopic analysis of fingerprints can benefit the forensic community by offering a means of identification and isolation of a latent print from its background that does not rely solely on physical means of development (i.e., one lacking descriptive chemical information). The narrow vibrational bandwidths of analyte molecules allows discernment of, for instance, a vibrational band of urea from a closely related vibrational band of the amide bonds in the wooden surface on which the print is deposited. Using chemical signatures to discern on-ridge from off-ridge would allow imaging of prints irrespective of chemical pre-treatment with fuming or dyes. Using the weak but perceptible Raman signature of amino acids and urea would ameliorate the need for oils within the print to preserve moisture and protect the lactate ion, a component proven in our earlier work to act as the main initiator in the polymerization of cyanoacrylate vapors.(3) Optical vibrational spectroscopic has previously been reported utilizing Fourier transform infrared (FTIR) spectroscopy to image latent prints on highly reflective surfaces and on tapes/gels using an attenuated total reflectance cell.(34) Reconstructed images comprise an intensity map of one or more regions of vibrational spectrum indicative of a fingerprint. However, the FTIR based spectral interrogation described does not utilize portable instrumentation, and IR in general suffers from water signal background to a greater extent than Raman. The work presented also conveys results on the technological background of surface enhanced Raman spectroscopy (SERS) chemical imaging. SERS is evaluated for creating a chemical image of latent prints by following a characteristic spectral signal from print components. Raman imaging data, illustrating the ability to co-identify contaminants within a print, i.e., drugs of abuse or explosive residue, is also presented.

Statement of hypothesis or rationale for the research

The hypothesis for this research is founded upon identifying components of fingerprints that persist and resist photo- and thermal degradation, with an understanding of what degradation products may grow in or become significant during the course of photo- or thermal exposures,

we can apply surface enhanced Raman spectral imaging as a vibrational imaging detection strategy that keys off of the components that are most prominent in a latent fingerprint that would otherwise go undetected using traditional techniques. The degradation of fingerprints is a recognized route to loss of evidentiary value, and the use of optical and even vibrational spectroscopy has been proven in the research literature as a potential approach to latent fingerprint detection.

II. Methods

Artificial Fingerprint Solution

In order to perform multiple sequential analyses on eccrine fingerprint material with the possibility of increasing concentrations of the components, an artificial fingerprint solution was identified and is discussed at length below in the section on fingerprint component degradation. Briefly, the process included a compilation and evaluation of literature recipes to yield an optimized single complete surrogate eccrine recipe. A reference was found that identified and quantified (in $\mu\text{moles/print}$) the individual amino acids and urea found in a thumbprint deposited on a glass surface.(13) The Geigy Scientific Tables were consulted for the non-amino acid composition of eccrine secretions, reported in mg/L .(9) Calculations were performed to correlate the amount of urea and total amount of all amino acids found in one print, as reported by Hamilton, with the overall concentrations of those substances found in eccrine sweat, as reported in the Geigy Scientific.(9, 13) According to the urea data, one print consisted of $23.92 \mu\text{L}$ of sweat; based on the amino acid data, one print contained $31.89 \mu\text{L}$ of sweat. The average of these values, $27.91 \mu\text{L}$ of sweat per print, was employed for all conversion calculations used to create a “recipe” for an artificial eccrine-fingerprint solution, shown in Table 2 below.

Table 2: Composition of Artificial Eccrine Fingerprint Solution

Components	mg/L (= µg/mL)	% Composition	Components	mg/L (= µg/mL)	% Composition
AMINO ACIDS:			FATTY ACIDS:		
Serine	399.21	7.16	Acetic acid	7.69	0.14
Glycine	191.00	3.42	Propionic acid	0.26	0.005
Ornithine (as Ornithine HCl)	205.46	3.68	Butyric acid	0.21	0.004
Aspartic acid	109.71	1.97	Isovaleric acid	0.11	0.002
Histidine	100.08	1.79	Hexanoic acid	0.10	0.002
Alanine	92.59	1.66	Isobutyric acid	0.07	0.001
Threonine	76.84	1.38			
Lysine	57.63	1.03	Urea	1180.00	21.15
Valine	54.58	0.98	Sodium chloride (NaCl)	1138.46	20.41
Leucine	51.71	0.93	Potassium chloride (KCl)	640.74	11.49
Glutamic acid (as monohydrate)	53.26	0.95	Lactic acid	616.00	11.04
Proline	45.38	0.81	Ammonium hydroxide (NH ₄ OH)	107.01	1.92
Phenylalanine	41.44	0.74	Calcium sulfate (CaSO ₄)	98.50	1.77
Tyrosine	38.96	0.70	Glucose	70.00	1.25
Isoleucine	37.61	0.67	Pyruvic acid	40.00	0.72
Arginine	31.21	0.56	Sodium sulfate (Na ₂ SO ₄)	24.92	0.45
Citrulline	25.11	0.45	Magnesium sulfate (MgSO ₄)	15.85	0.28
Methionine	10.69	0.19	Creatinine	4.60	0.08
Taurine	4.48	0.08	Zinc chloride (ZnCl ₂)	2.40	0.04
Cystine	0.72	0.01	Uric acid	2.02	0.04
α-Amino-n-butyric acid	0.36	0.01	Sodium bicarbonate (NaCO ₃ H)	1.45	0.03
			Acetylcholine iodide	0.1214	0.00218
			Histamine	0.0135	0.00024
			Sodium iodide (NaI)	0.0045	0.00008

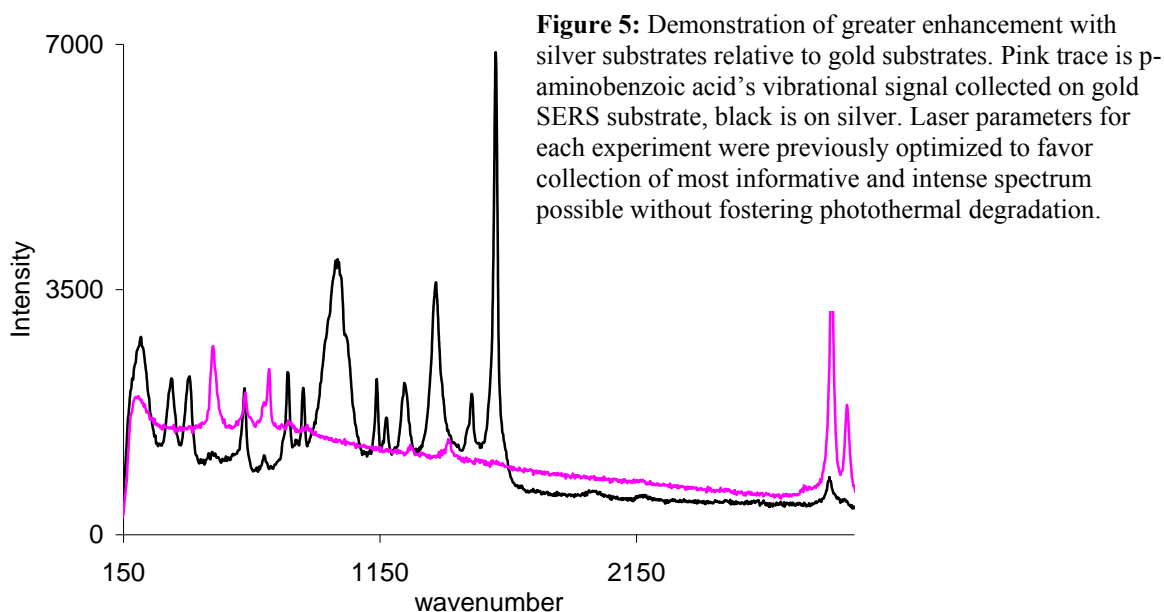
Raman Instrumentation and Chemicals

Several Raman instruments were used during the course of this developmental work. For initial surveys of SERS activity of individual fingerprint components with silver and gold nanocomposite substrates, a JYHoriba LabRam was used with a thermoelectrically cooled CCD detector, notch filter for rejection of Rayleigh scatter and laser line, and a 632.8 nm helium-neon laser. Laser power at-sample is 8.9 mW, and sample acquisitions were all set to 1 second, unless otherwise noted. For experiments with gold nanocomposite substrates, a Dilor Raman spectrometer was used that employed a triple monochromator wavelength selection with laser line rejection and a liquid nitrogen cooled CCD camera. Both of these instruments use versions of LabSpec software. Raman images were collected by co-authors R. Schuler and C. Gardner at ChemImage, Corporation's Pittsburgh, PA, USA, location on a FALCON® Microscope Raman and Fluorescence Imaging System while an ORNL prototype imager was being constructed. The FALCON® system utilizes a liquid crystal tunable filter (LCTF) for collected scattered wavelength selection. These systems also have a thermoelectrically cooled CCD. Raman chemical images are created by such a system as follows: the impinging laser light is expanded to 20 mm diameter, light is collected over a narrow wavelength range defined by the LCTF, and an image at essentially a single wavelength of Raman scattered light is created and stored. The LCTF then tunes to another wavelength and the process is repeated, stacking "single" Raman wavenumber images on top of each other until a hyperspectral cube is created. In this cube, the X and Y axes define an intensity map of the sample's Raman scatter signal at a particular wavenumber electromagnetic region. The Z direction illustrates the Raman spectrum from single spots once the cube is constructed via LCTF tuning across whatever wavenumber regions are defined by experimental parameters. The difference in this type of imaging as contrasted with conventional Raman rastering or mapping is the speed with which the image can be collected in a situation where the target analyte is known, and therefore a predetermined spectral region can be targeted by the LCTF. Conventional rastering or mapping creates a Raman image by collecting an entire Raman spectrum at each of many spots across the sample, after which the intensity map is reconstructed by following defined wavenumber regions from within the X – Y grid of whole spectra. This approach is more suitable for gaining descriptive information from maps of unknown substances as it is more time consuming than large field of view imaging using known wavenumber regions of interest for analytes, in our case fingerprint materials. For SERS response screening, 1mM solutions of the fingerprint components were prepared individually in 18MΩ deionized water from a Millipore Elix® system. All chemicals were procured from Sigma-Aldrich and used as received.

SERS Reagents and Nanoparticle Dispersal

Several incarnations of surface enhanced Raman substrates were employed, falling into three categories. (i) Advanced, non-dispersible substrates were used for proof-of-principle demonstrates supporting SERS chemical imaging of fingerprint material deposited directly onto the substrate. (ii) Conventionally prepared silver colloidal solutions were utilized for solution screening of eccrine fingerprint component chemicals at concentrations of 1×10^{-3} M, and diluted to 1×10^{-4} M when combined with colloid. Conventional colloids were also heavily used in early dispersal studies and solvent exchange tests. (iii) Finally, four types of advanced solution-based substrates were tested, of which only silver-coated gallium oxide nanowires yielded as sensitive or more sensitive SERS responses when compared with conventional colloid. Nanocomposites of silver metal vapor deposited onto the elastomer polydimethylsiloxane (PDMS) used in the initial proof of concept experiments were previously characterized by Sepaniak, et al.(35-38) The bulk Sylgard polymer was mixed in a 10:1 ratio with curing agent, degassed under vacuum, poured onto a 1"x3" microscope slide, and cured at 70°C for 1 hour. The slide was then inverted in a physical vapor deposition unit (PVD), and silver metal was deposited in a sublimed plume from a resistively heated tungsten boat at a pressure of 2×10^{-6} Torr. This substrate, although

beneficial in its solid phase extraction and slow silver oxidation characteristics, is non-dispersible and therefore not amenable to field use. Conventional silver colloidal solutions were used for screening the individual components of eccrine prints. These spherical particles were reduced with trisodium citrate or with sodium borohydride using silver nitrate as a feedstock with stirring at temperatures of 90°C and in an ice bath, respectively. Further details of these preparations have been exhausted in the literature.(39-41) Preparation of geometrically shaped silver nanoparticles for SERS enhancement included rods, cubes, triangular nanoprisms, and silver-coated dielectric core nanowires may also be found in the literature.(42-45) Only the nanowires possessing a dielectric core produced results equal or superior to the conventional colloid; thus, the material preparation is included herein. Dielectric core-metal shell nanowires were prepared at the Naval Research Lab via thermal vapor liquid solid deposition of Ga₂O₃ onto gold catalyst spots in a tube furnace.(45) Silver was vacuum sputtered onto the nanowires at a nominal thickness of 6nm. A full description and analysis of the nanowires' preparation and fundamental properties is available in Reference 33. Scanning electron micrographs of the triangular nanoprisms demonstrating their prohibitively dilute solutions were collected at the ORNL High Temperature Materials Laboratory on a HF3300 TEM/STEM operated at 300kV. The SEM of dielectric core-metal shell nanowires was collected by Sharka Prokes at the Naval Research Lab.



One area where the less active gold substrates (an example of the difference in SERS enhancement of silver versus gold for one representative compound is shown in Figure 5) still hold much promise is their chemical selectivity for nitrogenous compounds. Urea was chosen as an eccrine print surrogate for 780nm laser testing because, although not yielding so rich a SERS spectrum as some other eccrine or sebaceous components, it does have several reliable vibrational bands, most notably at 1100cm⁻¹ (a common band location with several of the sebaceous fatty acids) and 1250cm⁻¹, and also because it comprises 20% of the non-aqueous content of eccrine prints. Gold colloid with a predicted mean diameter of 12 nm and 24.5 nm proved most SERS active with both 633nm and 780nm lasers. These nanoparticle dispersions were created by adding 1.75 mL (for 12 nm particles) and 0.75 mL (for 24.5 nm particles) of 1% (w/v) Na₃citrate to an initial solution of 50 mL 0.01% (w/v) HAuCl₄. (41) The solutions go from grey to red to lavender in color over ~5min under open flask reflux with volume replacement. For single component analyses, colloid solution is applied to a pre-cleaned frosted glass slide via high performance nebulization with 2 mL colloid being applied over a slide area of 0.5 x 2 cm.

For sebaceous or eccrine fingerprint analysis in these tests, a cleaned, flat glass slide was used to collect a print. Colloid was sprayed over top of the print in the same manner as described previously for a frosted glass slide. Table 3 summarizes the slight deviation in preparation methods for the relevant gold colloid solutions and their resulting mean diameters of particles, in addition to brief comments about their SERS activities. The nebulizer that was used in these studies was from CETAC Technologies, Omaha, NE, USA.

Both 633nm and 780nm could be used for interrogating latent fingerprint components with the robust SERS substrates created by nebulizing gold nanoparticles onto said prints to create a directly applicable noble metal nanostructure that facilitates the enhancement of vibrational scattering and also may help quench competing fluorescence background. *However, it must be reiterated that these studies with gold have only highlighted the increased activity of silver as a SERS substrate, even at longer wavelengths.* A study was carried out on a Dilor Laboratory Raman spectrometer at 780nm to yield the preliminary information required to select the optimum laser source for the ChemImage macro-Raman imaging spectrometer system design. The power density for the Ti:sapphire laser in the Dilor Raman spectrometer was high relative to the targeted laser power density from a diode laser system, due mostly to a larger field of view with similar laser power for the fingerprint-specific imaging system. At a power density of $\sim 1800\text{W}/\text{cm}^2$ (9mW laser power coming out of the microscope objective spread across a circular area defined by a 25micron beam diameter), the urea spectra show one or two strong SERS lines around 1100cm^{-1} and 1280cm^{-1} , with three of the nine colloid solutions (all three were citrate reductions, with 12, 16, and 24.5 nm nominal particle diameters giving some signal). Of these three, the best was a preparation with a nominal nanoparticle diameter of 12nm. For the stated laser power, the max signal was ~ 2000 counts. We next moved forward with SERS studies on degradation products with chemical information within light and air exposed fingerprints, focusing on the components which show most SERS activity. What's more, all gold work can also be performed with silver colloidal preparations with illumination by the 633nm line of the Helium Neon laser Raman systems.

Volume Reductant Added	Particle Size Generated (nm)	Comments on SERS Activity
1.75 mL citrate	12 (best gold colloid at 633 and 780)	Active with both, better w/633
1.0 mL citrate	16	Active with both, better w/633
0.75 mL citrate	24.5	Active with both, better w/633
0.50 mL citrate	41	Vaguely active with both
0.30 mL citrate	71.5	Inactive
0.21 mL citrate	97.5	Inactive
0.16 mL citrate	147	Inactive
0.6 mL 0.1M borate	5.2	Inactive
0.6 mL 0.1M borate (at 4°C)	5.2	Vaguely active with 633nm

Table 3: Preparation methods for the gold colloid solutions used during SERS reagent studies and their resulting mean diameters of particles with comments on activity.

Dispersal solvent and method were important parameters to SERS reagent development. Two factors govern solvent selection: volatility and interaction with the metal nanoparticles. All solvents were HPLC grade and used as-is from the manufacturer, Fisher Scientific. Dispersal of nanoparticle solutions must be a nearly dry spray from an instrument that is field portable. The

dispersed nanoparticle solvent must meet two requirements: (1) high volatility to mitigate pooling which compromises SERS enhancement (due to over-aggregation of metal nanoparticles and prevent latent print wash-off or blurring) and (2) low Raman activity to promote negligible spectral background. Solvent exchange after SERS nanoparticle preparation is necessitated during the creation of nanoparticles due to the native aqueous citrate environment of some colloid synthesis, which is not conducive to collection of good SERS vibrational signals due to background signals from citrate and competition for loci of high optical field enhancement. An approach was developed wherein solvent matrices are easily changeable via one to three repetitions of a process that includes: (1) centrifugation followed by decanting off the water/citrate synthesis matrix; (2) adding methanol or acetone back up to volume; (3) followed by a second solvent replacement step with a yet more volatile solvent such as methyl acetate. This approach was crucial to the incorporation of a matrix that evaporates considerably faster than water into the SERS substrate delivery system. Faster evaporation facilitates SERS detection of latent prints by preventing solvent pooling and unfavorable agglomeration during SERS reagent application. Especially with less expensive, lower performance delivery tools used with highly polar or high evaporating solvents, the metal nanoparticles cluster in geometries unfavorable to maximum SERS enhancement. Another, equally important, reason to employ delivery solvents that do not allow excessive pooling is that some print material may be lost due to extensive soaking by the delivery solvent. **Table 4** contains a summary of some characteristics indicative of performance of the solvents for dispersal. A final consideration in choosing a more volatile nanoparticle delivery solvent is that the solvent must not chemically compromise the silver metal nanoparticles being imposed upon latent print containing surfaces by either binding to or oxidizing the silver.^{6,7} Methanol and acetone work equally well as delivery solvents for nonporous latent print containing surfaces, with acetone giving background bands for the carbonyl vibrational band and methanol evaporating somewhat more slowly but yielding no significant background bands. For this reason, methanol was used as the second in a rinse sequence that begins with aqueous colloid solution and ends with ethyl acetate as a delivery solvent in cases where the need for extremely quick evaporation arises, such as extremely unwettable (Teflon) or porous surfaces.

Delivery Solvent	Boiling Point	Polarity Index	Comments
Water	100°C	10.2	Slow evaporation can cause pooling
Ethyl Acetate	77°C	4.3	Minor reduction of SERS response
Methanol	65°C	5.1	Insignificant background
Acetone	56°C	5.4	Carbonyl bands give some background
Methyl Acetate	56°C	4.4	Evaporates quickly; minor reduction of SERS response
Diethyl Ether	35°C	2.8	Fast evaporation; flammable and dangerous if inhaled

Table 4: Characteristics of the solvent candidates utilized for delivery systems.

As for the dispersal instruments, the earliest trials utilized citrate or borohydride reduced conventional colloid, nanocubes, and triangular nanoprisms in aqueous matrices dispersed through a CETAC® high performance nebulizer. Next, a commercial grade airbrush by Pasqual® was employed. Finally, a commercially available aerosol propellant can (Preval®) made to interface with a refillable glass reagent bottle was utilized with non-aqueous dispersal solvents to form the current iteration of a field-ready implement for deploying SERS enhancing reagent onto surfaces containing latent fingerprint material. The high performance, expensive, and time intensive CETAC® nebulizer required compressed gas as a propellant. This system can disperse a wide range of solvents, with a water load up to 100%. The higher throughput airbrush required DC power, but did not require feed gas. This system can disperse SERS substrate solutions containing up to a 40% water load without over-wetting the target. The cheapest delivery system, required the most volatile dispersal solvents for SERS dispersal, such as ethyl acetate, with low concentrations of acetone or ethanol and only traces of water to prevent over-wetting. A completely novel spray apparatus was invented for applying SERS enhancing reagent by Sam A. Lewis of the ORNL team, shown in Figure 6. This unit eliminates the problem of

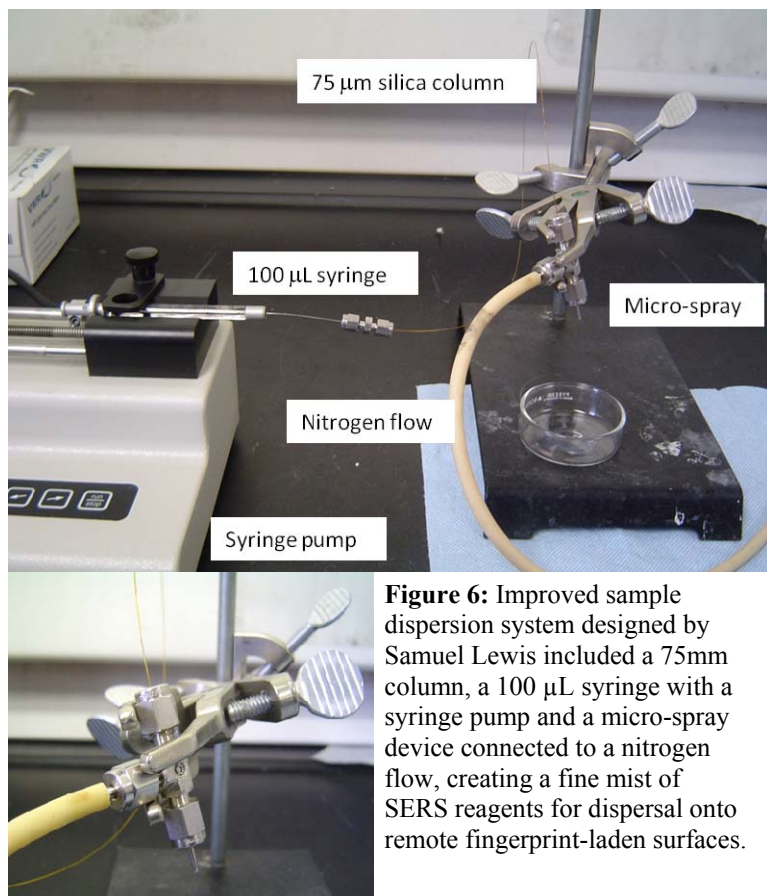


Figure 6: Improved sample dispersion system designed by Samuel Lewis included a 75mm column, a 100 μ L syringe with a syringe pump and a micro-spray device connected to a nitrogen flow, creating a fine mist of SERS reagents for dispersal onto remote fingerprint-laden surfaces.

delivery solvent pooling, allowing deposition of appropriate amounts of SERS enhancing reagent without overwetting the fingerprint. A moderately discernible, non-optimized image of a clean fingerprint was collected using the imager by applying silver-coated gallium oxide nanowire solution to the print on an aluminized glass slide. Improvements in delivery of the SERS reagent will allow more complete coverage and more sensitive chemical signal recovery while preserving the integrity of the fingerprint ridges. A major improvement of this type was realized with the implementation of an electro-spray-inspired pressure driven concentric flow of inert gas around a central stream of SERS enhancing nanowires solvated in methanol. This device results in coverage unmarked with drying spots

or pooling and represents a significant advancement toward ideal delivery of SERS enhancing reagents.

System Delivery

On the morning of May 20, 2008, the MCRIS was delivered to the laboratory of Mr. Samuel Lewis at the National Transportation Research Center, a part of Oak Ridge National Laboratory. Dr. Charles Gardner of ChemImage Corporation set up the instrument on an available lab bench as shown in Figure 7. Figure 8 shows an image of the test chart at the specified 20 mm field of view. Figure 9 shows the full-range acetaminophen spectrum acquired on the system along with the brightfield and Raman images. Alignment of the brightfield illumination and the laser illumination was verified and an auxiliary fan was installed to improve the temperature stability of the tunable filter. On May 21, 2008 a new laser rejection filter was installed in the system in an attempt to improve the performance in the low wavenumber range.

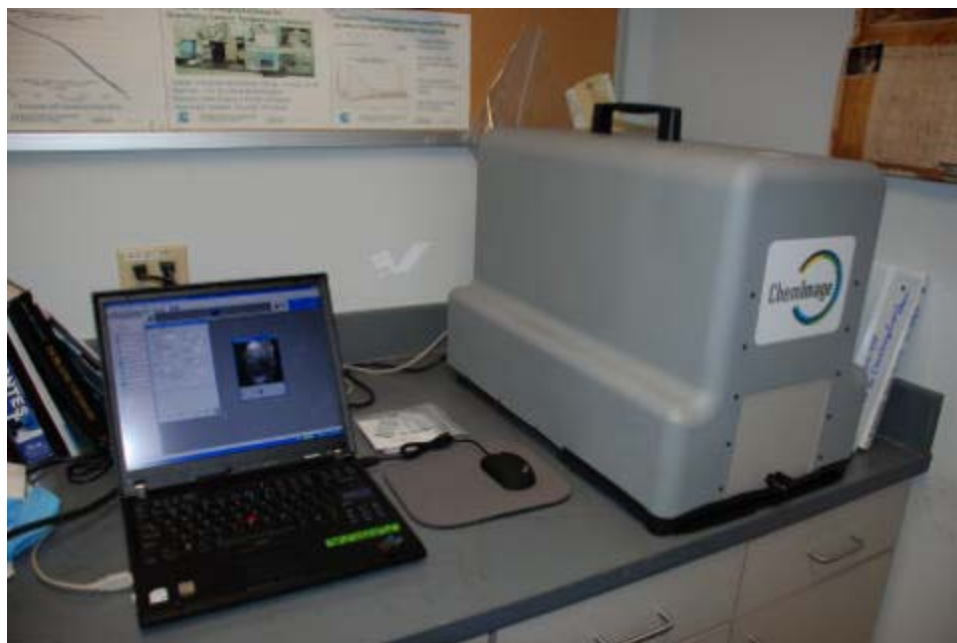


Figure 7. Macro Raman Chemical Imaging System Installed at Oak Ridge National Laboratory. After set up, both the imaging performance and the spectral performance of the system were evaluated.

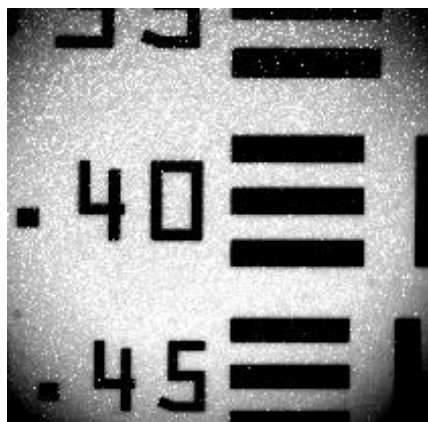


Figure 8. Image of Test Chart taken with the Macro Raman Chemical Imaging System. Numbers are the line spacing in lines/mm.

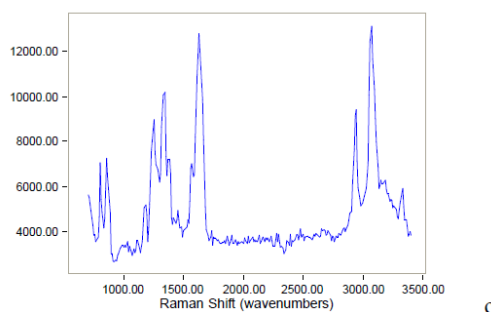
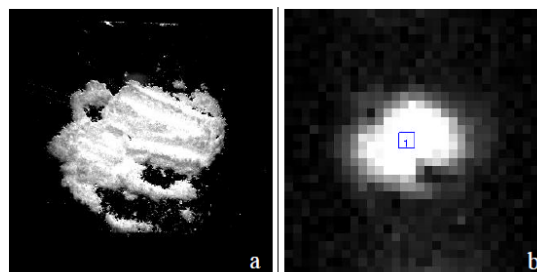


Figure 9. Full-Range Acetaminophen Spectrum taken with the Macro Raman Chemical Imaging System. a) Brightfield image b) Raman image at 1620 cm^{-1} c) Average Raman spectrum within rectangle.

System Software Training

On May 21 and 22, 2008, R.M. Connatser was trained on the operation of the MRCIS and on the use of the ChemImage Xpert™ software package which provides instrument control as well as image acquisition and analysis. The training covered the following topics: instrument start up, camera operation, tunable filter operation, laser operation and safety, zoom lens operation, brightfield imaging, acquisition of spectral data sets, acquisition of Raman Chemical Imaging data sets, selection of regions of interest (ROI), and overlay of acquired spectra.

Methods for Photo and Thermal Degradation Studies

Artificial Eccrine Fingerprint Standards

Hamilton's quantitative data of the individual amino acids plus urea found in an eccrine-only thumbprint (13) was combined with reference data from the Geigy Scientific Tables on eccrine sweat secretions (9) to create a 44-component artificial eccrine fingerprint solution (Table 1). After screening the individual component chemicals for ease of detection by surface enhanced raman spectroscopy (SERS) (46) for a correlating degradation studies discussed in another publication, the following SERS-active components were chosen for further study: aspartic acid, glutamic acid, glycine, histidine, ornithine, serine, threonine, urea, and lactic acid. Aqueous fingerprint standards were made of each amino acid at five times its single-print concentration, a mixture of all seven amino acids at five times their single-print concentrations, urea at 100 times its single-print concentration, and lactic acid at 100 times its single-print concentration. All amino acids (DL-aspartic acid, DL-glutamic acid monohydrate, glycine, DL-histidine, L-ornithine HCl, DL-serine, DL-threonine) and urea were purchased from Aldrich (Milwaukee, WI) at purity levels of greater than 98%; lactic acid (an 88% racemic mix in water) was purchased from Mallinckrodt (Phillipsburg, NJ). To prevent bacterial growth contamination of these standards, all solutions were biologically sterilized by filtering through 0.1 μm -pore size, 32mm-diameter acrodisc sterile syringe filters with Supor membrane (Pall Corporation, East Hills, NY). The solution containers were flame sterilized. All sterilization procedures were carried out in a biological hood.

Photo-Degradation Studies

Using gas-tight syringes for precise volume control, 28 μL (equivalent to the standard volume of material in one fingerprint, based on calculations from data in 1,2) of the individual 5X amino acid standards were deposited on separate sets of seven Teflon® discs (22mm-diameter) and seven steel coupons (19.6mm x 15.8mm x 4.4mm), for a total of 98 amino acid samples. The samples were allowed to dry overnight in the dark, before being exposed to a 200-500 Watt Xe/HgXe Arc Lamp intense light source (Oriel Corporation Model 87301, Stratford, CT) for periods of time equivalent to 0, 2, 5, 7, 14, 28, and 56 days. The light source emits visible, UV-A, UV-B, and UV-C wavelengths, simulating 365 days of sunlight exposure in 24 hours of lamp use (see Table 2 for the lamp exposure times that correlated with the desired duration of continuous sunlight exposure). The same sample preparation procedure was repeated with the 100X urea and 100X lactic acid standards, for an additional 28 samples. Teflon discs were reused throughout the study, with a multi-step cleaning with lab soap, distilled water, acetonitrile, and methanol between each use. Steel coupons were used only once.

Thermal-Degradation Studies

Thin galvanized steel coupons (15.7mm x 15.7mm x 0.5mm) were cleaned with acetonitrile and methanol to remove lubrication oils used in the coupon-cutting process, sanded with 4000-grit (or better) sandpaper to remove any possible surface oxidation, and wiped again with acetonitrile and methanol. Using gas-tight syringes for precise volume control, 28 μL of the 5X standard amino acid mixture was deposited on four steel coupons. The samples were allowed to dry overnight in the dark. A commercially-available 120-V, 1200-W heat gun (Black&Decker Model No. 9756, Hunt Valley, MD) was turned on to the "high" setting for at least three minutes. A vise-grip clamp was used to grasp a steel coupon along its edge and suspend it directly over the heat gun, with the non-deposited side facing the heat source. A thermocouple (Omega Engineering, Stamford, CT) in contact with the steel coupon measured the temperature experienced by the side spotted with the fingerprint sample. Once the desired temperature was achieved an estimated time of exposure should be given to demonstrate the attempt of rapid heating (50°C, 100°C, or 150°C) the steel coupon was immediately removed from the heat source and allowed to cool on a wire rack for three minutes. The fourth coupon was not heated, to be used as the ambient reference. The thermal degradation procedure was repeated with the 100X urea and 100X lactic acid standards.

Amino Acid Sample Analysis

The amino acid samples were placed face-down in glass vials containing 1 mL of a 50 mM aqueous solution of sodium dodecyl sulfate (Fluka, Seelze, Germany); then the vials were placed in an ultrasonic bath for 30 min to promote extraction. The solvent was recovered and taken through the “EZ:faast™ for Free Physiological Amino Acid Analysis by LC-MS” derivatization kit (Phenomenex, Torrance, CA). This EZ:faast™ sample derivatization consisted of the introduction of a mixture of three internal standards and a solid phase extraction utilizing amino acid-trapping sorbent particles, followed by the proprietary derivitization and a liquid/liquid extraction. The organic liquid layer was evaporated to dryness under nitrogen then reconstituted in 100 μL of a 2:1 (v/v) mixture of 10 mM ammonium formate (Fluka, Seelze, Germany) in MeOH and 10 mM ammonium formate in H₂O. Samples were analyzed by liquid chromatography coupled to positive-ion electrospray mass spectrometry using an Agilent (Wilmington, DE) 1100 Series LC instrument and Bruker Daltonics (Billerica, MA) Esquire-LC MS instrument with settings as presented in Table 3.

Urea and Lactic Acid Sample Analysis

The urea and lactic acid samples were placed face-down in glass vials containing 5 mL of MeOH:H₂O (1:1, v/v) with 0.15% formic acid (JTBaker Inc., Phillipsburg, NJ). The vials were placed in an ultrasonic bath for 30 min to promote extraction. The solvent was removed and filtered through 0.1 μm Supor-membrane sterilized filters (Pall Corporation, East Hills, NY). Urea samples used an internal standard of 10 ppm of melamine (as melamine 99%, Aldrich, Milwaukee, WI); lactic acid samples used an internal standard of 10 ppm of cyanuric acid (Aldrich, Milwaukee, WI). Melamine and cyanuric acid were dissolved in MeOH:H₂O (1:1, v/v) with 0.15% formic acid at a final concentration of 20 ppm. For urea samples, 100 μL of the extracted solution was spiked with 1 mL of internal standard solution and 900 μL of blank extraction solvent. For lactic acid samples, due to the low intensity of the signal, 200 μL of the extracted solution was spiked with 1 mL of internal standard solution and 800 μL of blank extraction solvent. The samples were then analyzed by direct infusion at 2181 μL/h into an atmospheric pressure chemical ionization mass spectrometer (APCI-MS) using a Bruker Daltonics (Billerica, MA) Esquire-LC MS instrument with settings as presented in Table 4. Due to the high background of the cyanuric acid for the lactic acid sample determination, the analysis was conducted adopting a 4-port switching valve. For each analysis the sample was injected twice for 24 seconds. An infusion of blank solvent extraction at a rate of 4 mL/h was constantly used between sample injection and each run.

III. Results and Discussion of Findings

Surface enhanced Raman shows promise for chemical imaging of latent prints (either eccrine or sebaceous in nature), as well as print contaminants and daughter products of print degradation, such as the pyruvic acid that grows in and then itself degrades as lactic acid degrades. (47) The current time to image a single print is 30 seconds based on the narrow vibrational band at 1129 cm⁻¹ or 2900 cm⁻¹ and 10-30 minutes to create a full spectral profile of the print. In our SERS substrate development, this procedure is common practice to fully characterize the substrate’s performance and look for any potential contaminants. In the field/forensic lab setting, this long acquisition time would only be employed if unknowns were suspected and the practitioner desired vibrational information to use in an attempt to identify non-fingerprint materials. The data represented in Figures 2, 3, and 10 illustrate how Raman chemical imaging, using the hydrocarbon band from skin oils at 2900 cm⁻¹ can be used to create a detailed picture of a fingerprint and possible contaminants therein. Although the SERS chemical image collected in Figure 2 was of a fingerprint placed onto an elastomer-metal nanocomposite SERS substrate, a print collection geometry unusable for latent prints, the

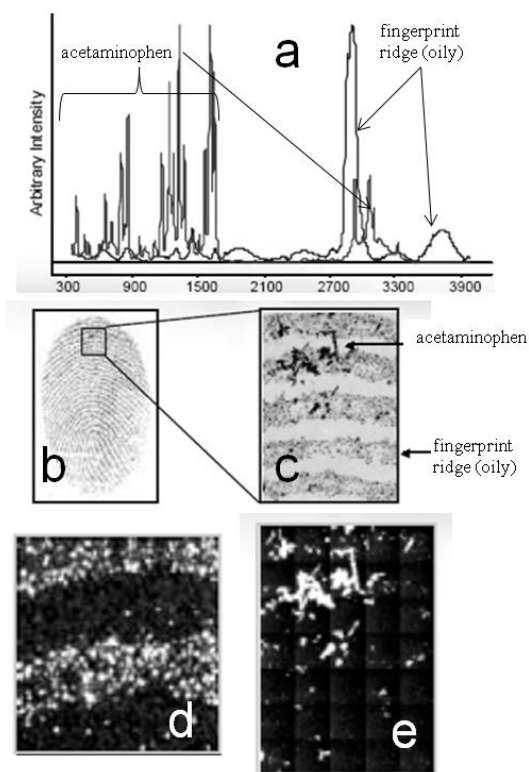


Figure 10: Raman chemical imaging of a sebaceous fingerprint doped with acetaminophen and placed on a clean, highly reflective slide. (a) Overlaid Raman spectra of fingerprint oil and acetaminophen to represent potential drug-related latent print contaminants. (b) 1.25x magnification of brightfield image of print/drug. (c) 5x magnification of zoom camera brightfield image of region of print/drug. (d) 20x magnification Raman chemical image montage of fingerprint ridges, 2900 cm^{-1} image extract. (e) 5x magnification of Raman chemical image of acetaminophen on fingerprint, 2940 cm^{-1} image extract.

chemical image created serves as a formidable proof that sufficiently sensitive dispersible SERS substrates could facilitate print imaging on remote evidentiary surfaces. Figures 3 and 10 describe a conventional Raman image of fingerprint oils and added pharmaceutical dust (acetaminophen) deposited directly onto a completely clean, highly reflective surface to demonstrate the capability of vibrational spectroscopy for discerning latent prints from informative contaminant spectra. The phenomenon of surface enhancing Raman scatter is necessary to increase the scattering efficiency of fingerprint components to the point that scatter can be detected from light or partial prints, heat or photodegraded prints, as well as from non-ideal remote surfaces or dielectric environments. Enhancement is achieved by introducing analyte into close proximity with a roughened metal surface or clusters of noble metal nanoparticles. Interaction with impinging laser light initiates a coherent oscillation parallel to the surface in the valence electrons of the metal. These plasmon bands enhance both the electromagnetic fields impinging on and scattered by the analyte molecules.⁽¹⁸⁾ Chemical effects, such as electrostatic, steric, or even covalent bonding can alternately improve the enhancement via charge transfer fluorescence quenching. By the same token, the enhancement factor can be compromised by the chemical effect when analyte molecules are

effectively excluded from electromagnetically favorable loci among the nanoparticles or nano-roughness of a metal surface. This chemical inhibition of SERS enhancement makes selection of a dispersal solvent critical. It was found that a regime to remove SERS active nanoparticles from their native aqueous solution and into a more volatile solvent via incremental increases in solvent polarity alleviated spectral background due to residual reductant and facilitated better dispersal characteristics. Solvent exchange steps included centrifugation to gravitationally concentrate the particles into a small volume of their original water-based synthesis solution. This step was followed by sonication to achieve mixing into clean, deionized water free of reductant residuals. This water rinse was repeated, and after removing the second rinse, ethanol was introduced as the sonication solvent. The particles were then centrifuged for removal from the ethanol and introduced into ethyl acetate, which served as the final dispersal solvent. The resulting solution was approximately 25% ethanol, and 75% ethyl acetate with traces of water. This solution dissipated the nanoparticles onto test surfaces without pooling while maintaining ample wetness to prevent the dangers of aerosolized metal nanoparticles.

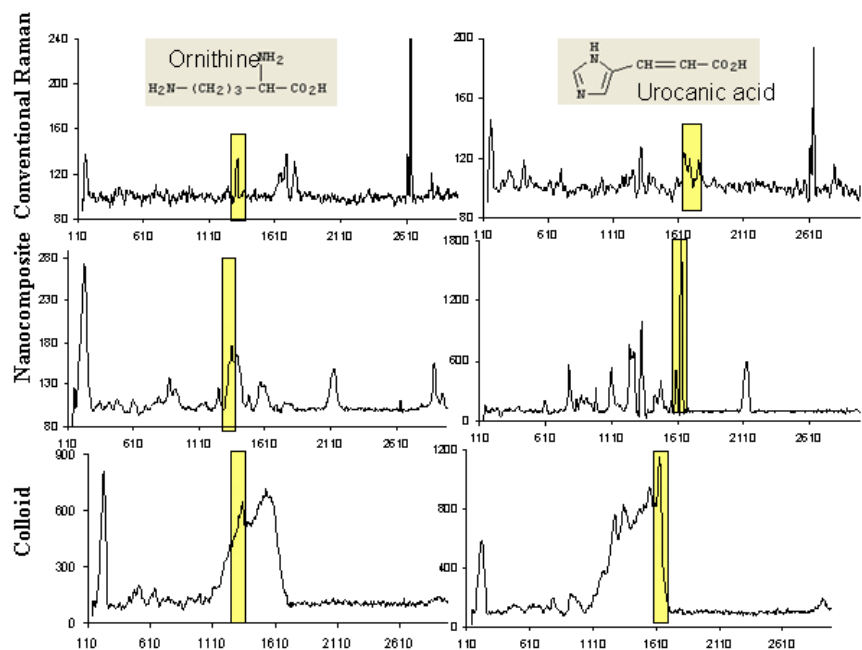


Figure 11: Activity for fingerprint components using conventional Raman, silver-elastomer nanocomposite and silver colloid substrates. Sample concentrations were neat, $1 \times 10^{-5} \text{M}$, and $1 \times 10^{-4} \text{M}$, respectively. Vibrational bands highlighted by box are distinctive to each analyte across substrate types.

SERS uses a myriad of different metal-dielectric combination substrates, including nanocomposites of polymer and metal, solution-prepared metal colloids of varied geometries, and sol-gel materials in fluid clusters or adsorbed on flat surfaces. Figure 11 illustrates several points relevant to discussion. First, the magnitude of conventional Raman signal for neat fingerprint components is easily matched by using surface enhanced Raman for solutions of components orders of magnitude lower in concentration ($1 \times 10^{-5} \text{M}$ with silver-elastomer nanocomposite and $1 \times 10^{-4} \text{M}$ with colloid). The highlighted vibrational regions indicate how, despite different vibrational broadening effects due to substrate adsorption and analyte molecule orientation, common vibrational signatures can be followed from Raman to different surface enhancing substrates. For the practical purpose of imaging latent fingerprints, the employment of dispersible Raman enhancing metal nanoparticle systems is required. Micrographs of the dispersible SERS substrates studied for latent print analysis are shown in Figure 12, and were collected with scanning or tunneling electron microscopes. Microscopy has the great benefit of revealing morphology of SERS substrates after they have been dispersed, crucial information to a technique that relies on particle spacing for efficacy. Even a cursory evaluation of the contrast between 12b with 12a and the inset SEM in 12c reveals one cause for lack of sensitivity of the dispersed advanced materials: spacing. Even long periods of dispersal (30 minutes to cover a square inch) of triangular nanoprisms do not yield the dense cross-covered nanoparticle layer necessary to yield sensitive, uniform image-creating enhancements.

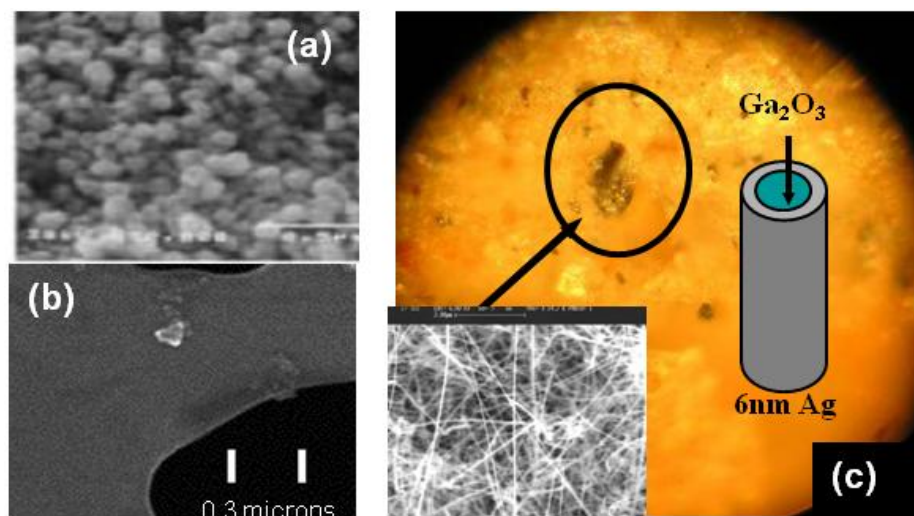


Figure 12: Comparison of dispersible SERS substrates. (a) Conventional silver colloid deposited onto glass using a droplet nebulizer. (b) Advanced substrate, solution-prepared triangular nanoprisms, dried from a droplet onto SEM mesh. (c) Gallium oxide nanowires coated with silver and dropped onto PVC that was previously coated with 5x concentrated eccrine fingerprint solution. Inset shows coverage within aggregates on the nanoscale superior to (b) and equal to (a), but micro- and milli-scale coverage is still insufficient for imaging latent prints.

The advantages in increased Raman enhancement purported for the geometrical nanoparticles in their respective synthetic reports relative to the conventional spherical colloid were not realized in our studies. The nanowires did, however, demonstrate a potentially higher response factor despite being too diffuse to facilitate collection of a complete fingerprint image. We speculate that the loss of Raman signal enhancement factor relative to original investigators' reports of sensitivity is due to the process of dispersal itself. For SERS reagents usually tested in solution or tethered to a surface in a self-assembled monolayer, the process of dispersal would render individual nanoparticles too far from each other for enhancement or in an unfavorable dielectric environment such as a solvent cage. This comparison of dispersible SERS substrates shows conventional silver colloid deposited onto glass using a droplet nebulizer, 12a, and gallium oxide nanowires coated with silver and dropped onto a surface, 12c, as giving greater coverage than the advanced substrate in 12b, solution-prepared nanotriangular prisms, also dried from a droplet. The inset shows coverage within aggregates on the nanoscale superior to 12b and equal to 5a, but micro- and milli-scale coverage is still insufficient for imaging complete or even partial latent prints. Also shown above in Figure 1a is the result that, despite being unable to image, we have achieved the collection of a SERS spectrum from an aggregate of nanowires on a porous galvanized metal pipe that was previously coated with 5x concentrated eccrine fingerprint solution. Such an aggregate is shown in the 80x magnified microscope picture in Figure 12c, along with an SEM of an aggregate of nanowires and a schematic depicting nanowire make-up. The absolute magnitudes of signal intensity cannot be compared between the spectra from conventional colloid (Figure 1a) and a nanowire aggregate (Fig. 1b), due to the collection at different impinging wavelengths (633 nm for Fig. 1a, 532 nm for Fig. 1b) on different instruments. Nonetheless, the response from the artificial solutions indicates promise in the optimization of the nanowires for higher surface coverage and extension of the nanowires' improved signal to noise in the detection of real prints. Currently, however, the conventional spherical colloid works best for our purposes because it can be prepared and sprayed in much higher particle densities for better surface coverage with similar enhancements. SERS screening was conducted on eccrine fingerprint components in an effort to assess these individual compounds for their contribution to the total vibrational scatter signals from the prints. Two separate facts led to this choice of eccrine screening. First, the absence of oils to retain moisture and slow photo-degradation of the lactate anion results in eccrine prints being the most difficult to retrieve. Second, since SERS is used in protein analysis to detect amino acids, we hypothesized that this technique could also be used to detect amino acids and other eccrine print components. This focus on clean (i.e., not oily), pure eccrine prints is not so much a requirement of this niche technique, it is a demonstration that during development researchers are targeting the more difficult of the two types of prints for detection. In fact, some of the most common

contaminants (blood, drugs, explosives) are actually easier to detect than the eccrine fingerprint constituents themselves. Several of the initial test solutions, all at $1 \times 10^{-3} \text{M}$ concentration in deionized water, yielded some vibrational bands when assayed on silver as well as gold nanocomposite. Table 1 enumerates all the vibrational bands and likely structural assignments detected for individual components of fingerprints in water.(15, 16) Bands in italics were detectable above the level of noise only with silver substrates, even when the wavelength of the Raman initiating laser was chosen to better align with gold substrates at 785 nm. However, none of the print components yielded spectra from gold substrates that even approached the response of the components on silver. Although using the SERS signature of aggregate surface amino acid moieties is well-established in the literature for discerning protein conformational changes, amino acids tend to give weak to modest SERS response when deposited onto a surface in high micromolar total amino acid concentrations as in latent fingerprints. None of the print components yielded spectra from gold substrates, at either wavelength, that approached the response obtain when employing silver. These results indicate that, with sufficient coverage by high Raman enhancement factor nanoparticles dispersed without chemical inhibition onto surfaces with latent prints, SERS chemical imaging should be possible.

IV. Conclusions

This work fills an important niche for chemically imaging clean, aged or new, latent fingerprints, especially on difficult surfaces or exposed to conditions that would render a latent print undetectable using traditional print development techniques. In order to continue progress on this effort beyond the proof-of-concept and process development steps reported herein, our on-going work targets the macro-Raman instrument design, testing, and especially further SERS reagent optimization for latent-print detection applications. A distinction of surface enhanced Raman imaging relative to FTIR imaging reports and other, more conventional methods of print visualization is that the amino acids in eccrine fingerprints can be targeted, instead of relying on the response or reactivity of oils' common hydrocarbon signal being used to create the image. The differences between FTIR and SERS imaging emerge in an examination of the background and reflectivity requirements of infrared imaging. Although the Fourier transform math can alleviate much of the background created by moisture in the vibrational absorbance spectrum, some sensitivity is lost in the averaging. What's more, the most compelling fingerprint images have been collected from highly reflective surfaces such as aluminum cans and surfaces that do not create a broad IR background including some polymers. Our technique seeks to address porous or granular surfaces, especially those marred during thermal events. The narrow Raman bands allow slightly more straightforward spectral identification and subtraction of polymer background bands without loss of analyte information. Finally, the surface enhancement phenomenon does not benefit IR absorption, so the only mechanism of increasing optical signal collected is longer image acquisition times, more powerful lamps, or IR tagging of fingerprint constituents. Future work will specifically improve the degree of Raman enhancement for urea and amino acids. Thereby, the ridge/furrow contrast, fingerprint chemical content, and ridge detail may be improved for an increase in sensitivity of the SERS chemical imaging technique.

Implications for policy and practice

Via conversations with collaborator Officer Timothy Schade of the Knoxville Police Department, we learned which surfaces most commonly contain latent prints, some of which are sometimes difficult to visualize fully with conventional print development methods due to surface chemistry and/or porosity effects. These include plastics (bags, wraps, polymer gun handles, non-adhesive side of duct tape), wood (both finished and untreated), and metal surfaces exposed to extreme heat after having a latent print deposited on them (shell casings, improvised explosive devices). Representative surfaces from each of these groups were tested with the SERS substrate delivery system described above. It was found that the increased evaporation speed of

acetone and methanol as SERS metal nanoparticle delivery systems worked best on all realistic surfaces tested (treated hammer handle, non-adhesive side of duct tape, black plastic garbage bag, Saran® wrap, aluminum metal) except such macroscopically porous surfaces as paper, cardboard, and untreated natural wood. Because these surfaces absorb the water when it is used as a delivery solvent, more SERS enhancing colloidal solution had to be deposited, but the water soaking into these absorbent surfaces seemed to benefit the collection of SERS signal from them. One obstacle that was under careful examination was the reduction in SERS signal from test surfaces to realistic surfaces. This difference was minimized with the realization that porous surfaces need a greater volume of colloidal solution deposited on them to achieve the same metal nanoparticle coverage attained with less deposited volume on flat, smooth, or less porous surfaces. Background bands from some substrates such as typing paper which contain large amounts of conjugated bleach and dye molecules will also require considerable careful analysis in order to see print vibrational components over such a complicated background. This type of analysis is quite feasible, though, especially since vibrational bands are generally narrow, reproducible in their relative wavenumber location, and therefore can be well defined as background or analyte bands.

The *major impediment to immediate progress* from lab to field is the unavailability of dispersible SERS substrates that retain adequate enhancing power, which facilitates sensitivity, upon dispersal onto remote surfaces where latent fingerprints are located. This area is currently under development in our laboratory. Further research will be focused on improving both the sensitivity and the broader, off-the-bench imaging capabilities of the technique.

V. References

1. Richmond-Aylor A, Bell S, Callery P, Morris K. Thermal degradation analysis of amino acids in fingerprint residue by pyrolysis GC–MS to develop new latent fingerprint developing reagents. *J Forensic Sci*, 2007;52(2),380-382.
2. Chiavari G, Galletti GC. Pyrolysis-gas chromatography/mass spectrometry of amino acids. *J Anal Appl Pyrolysis*, 1992;24,123-137.
3. Lewis LA, Devault G. Technology development, Enhanced latent fingerprint detection in missing and exploited children investigations. Final Report. 2004.
4. Lee, HC and Gaensslen, RE. Methods of Latent Fingerprint Development. In: Lee HC, Gaensslen RE, editors. *Advances in fingerprint technology*, 2nd edition. Boca Raton: CRC Press, 2001; 105-175.
5. Lewis LA, Smithwick RW, DeVault GL, Bolinger B, Lewis SA. Processes Involved in the Development of Latent Fingerprints using the Cyanoacrylate Fuming Method. *J For Sci* 2001; 46(2):241-246.
6. Wargacki SP, Lewis LA, Dadmun MD. Understanding the chemistry of the development of latent fingerprints by superglue fuming. *J For Sci* 2007; 52(5):1057-1062.
7. Wargacki SP, Lewis LA, Dadmun MD, “Enhancing the quality of aged latent fingerprints developed by superglue fuming: Loss and replenishment of initiator,” *Journal of Forensic Sciences* 2008; 53(5):1138-1144.
8. Ramotowski RS. Composition of latent print residue. In: Lee HC, Gaensslen RE, editors. *Advances in Fingerprint Technology*, 2nd ed. Washington, D.C.: CRC Press, 2001;63-104.
9. Sweat. In: Lentner C, editor. *Geigy Scientific Tables. Volume I: Units of Measurement, Body Fluids, Composition of the Body, Nutrition*. 8th rev. ed. West Caldwell, New Jersey: Ciba-Geigy Limited, 1981;108-112.
10. Bernier UR, Kline DL, Barnard DR, Schreck CE, Yost RA. Analysis of human skin emanations by gas chromatography/mass spectrometry. 2. Identification of volatile

- compounds that are candidate attractants for the yellow fever mosquito (*Aedes aegypti*). *Anal Chem*, 2000;72(4),747-756.
11. Mong GM, Petersen CE, Clauss TRW. Advanced fingerprint analysis project. Fingerprint constituents. PNNL Report 13019,1999.
 12. Asano KG, Bayne CK, Horsman KM, Buchanan MV. Chemical composition of fingerprints for gender determination. *J Forensic Sci*, 2002;47(4),805-807.
 13. Hamilton PB. Amino-acids on hands. *Nature*, 1965;205(4968),284-285.
 14. Noble D. Vanished into thin air: the search for children's fingerprints. *Anal Chem* 1995;67:A435-A438.
 15. Moskovits M, Suh J. Surface-enhanced Raman-Spectroscopy of amino-acids and nucleotide bases adsorbed on silver. *J Amer Chem Soc* 1985; 107(34): 6826-6829.
 16. Socrates, G. *Infrared and Raman Characteristic Group Frequencies*, 3rd Ed. Chichester: John Wiley & Sons, Ltd., 2001; pgs. 51, 53, 107-109, 125, 129, 132, 143-144, 151-152, 157-161.
 17. Fang HL, DaCosta FH, (Cummins Inc.). "Thermolysis Characterization of Urea-SCR". Workshop presentation at the Diesel Engine-Efficiency and Emissions Research (DEER) Conference; 2002; San Diego, CA, USA.
 18. Kneipp J, Kneipp H, Kneipp K. SERS - a single-molecule and nanoscale tool for bioanalytics. *Chem Soc Rev* 2008; 37(5): 1052-1060.
 19. Colthup NB; Daly LH; Wiberly SE. *Introduction to Infrared and Raman Spectroscopy*. Academic Press. New York: 1975. pp. 1-2.
 20. Andersen PC, Rowlen KL. Brilliant optical properties of nanometric noble metal spheres, rods, and aperture arrays. *Appl Spec* 2002; 56(5):124A-135A.
 21. Champion, A. and Kambhampati, P. *Chem. Soc. Rev.* 1998, 27, 241-250.
 22. Bell SEJ, Fido LA, Sirimuthu NMS, Speers SJ, Peters KL, Cosbey SH. Screening tablets for DOB using surface-enhanced Raman spectroscopy. *J For Sci* 2007; 52(5): 1063-1067.
 23. White PC. In situ Surface Enhanced Resonance Raman Scattering (SERRS) spectroscopy of biro inks - long term stability of colloid treated samples. *Science & Justice* 2003; 43(3): 149-152.
 24. Noonan KY, Beshire M, Darnell J, Frederick KA. Qualitative and quantitative analysis of illicit drug mixtures on paper currency using Raman microspectroscopy. *Appl Spec* 2005; 59(12): 1493-1497.
 25. Edwards HGM, Domenech-Carbo MT, Hargreaves MD, Domenech-Carbo A. A Raman spectroscopic and combined analytical approach to the restoration of severely damaged frescoes: the Palomino project. *J Raman Spec* 2008; 39(4): 444-452.
 26. Shi J, Li T, Feng M, Mao Z, Wang C. Study of the corrosion from the printing plates of 'Guan Zi' by Raman spectroscopy. *J Raman Spec* 2006; 37(8): 836-840.
 27. Grosserueschkamp M, Friedrich MG, Plum M, Knoll W, Naumann RL. Electron transfer kinetics of Cytochrome c probed by time-resolved surface-enhanced resonance raman spectroscopy. *J Phys Chem B* 2009; 113(8): 2492-2497.
 28. Han HWA, Yan XL, Dong RX, Song W, Yang M. Analysis of serum from type II diabetes mellitus and diabetic complication using surface-enhanced Raman spectra (SERS). *Appl Phys B-Lasers and Optics* 2009; 94 (4): 667-672.
 29. Chowdhury MH, Gant VA, Trache A, Baldwin A, Meininger GA, Coté GL. Use of surface-enhanced Raman spectroscopy for the detection of human integrins. *J Biomed Optics* 2006; 11(2): 024004.
 30. Day JS, Edwards HGM, Dobrowski SA, Voice AM. The detection of drugs of abuse in fingerprints using Raman spectroscopy I: latent fingerprints. *Spectrochim Acta A*; 60(3): 563-568.

31. Sapse D, Petraco NDK. A step on the path in the discovery of new latent fingerprint development reagents: substituted Ruhemann's purples and implications for the law. *J Molec Modeling* 2007; 13(8): 943-948.
32. Legendre M, Pochet N, Pak T, Verstrepen KJ. Sequence-based estimation of minisatellite and microsatellite repeat variability. *Genome Research* 2007; 17(12): 1787-1796.
33. Iqbal F, Hadjidj R, Fung BCM, Debbabi, M. A novel approach of mining write-prints for authorship attribution in e-mail forensics. *Digital Investigation* 2008; 5(Suppl.1): S42-S51.
34. Grant A, Wilkinson TJ, Holman DR, Martin MC. Identification of recently handled materials by analysis of latent human fingerprints using infrared spectromicroscopy. *Appl Spec* 2005; 59(9): 1182-1187.
35. Connatser RM, Riddle LA, Sepaniak MJ. Metal-polymer nanocomposites for integrated microfluidic separations and surface enhanced Raman spectroscopic detection. *J Sep Sci* 2004; 27(17-18): 1545-1550.
36. Connatser RM, Cochran M, Harrison RJ, Sepaniak MJ. Analytical optimization of nanocomposite surface-enhanced Raman spectroscopy/scattering detection in microfluidic separation devices. *Electrophoresis* 2008; 29(7): 1441-1450.
37. Giesfeldt KS, Connatser RM, De Jesus MA, Lavrik NV, Dutta P, Sepaniak MJ. Studies of the optical properties of metal-pliable polymer composite materials. *Appl Spec* 2003; 57(11): 1346-52.
38. Giesfeldt K, Connatser RM, De Jesus MA, Dutta P, Sepaniak MJ. Gold-polymer nanocomposites: studies of their optical properties and their potential as SERS substrates. *J Raman Spec* 2005; 36(12): 1134-1142.
39. Munro CH, Smith WE, Garner M, Clarkson J, White PC. Characterization of the surface of a citrate-reduced colloid optimized for use as a substrate for surface-enhanced resonance Raman-scattering. *Langmuir* 1995; 11(10): 3712-3720.
40. Keir R, Sadler D, Smith WE. Preparation of stable, reproducible silver colloids for use as surface-enhanced resonance Raman scattering substrates. *Appl Spec* 2002; 56(5): 551-559.
41. Hayat MA, Ed. *Colloidal Gold: Principles, Methods, and Applications, Volume 1*. San Diego, CA, USA: Academic Press, Inc., 1989.
42. Ibrahim A, Oldham PB, Stokes DL, Vo-Dinh T, Loo, BH. A comparison of enhancement factors for surface-enhanced Raman scattering using visible and near-infrared excitations. *J Molec Structure* 2005; 735: 69-73.
43. Sherry LJ, Chang S, Schatz GC, Van Duyne RP, Wiley BJ, Xia Y. Localized surface plasmon resonance spectroscopy of single silver nanocubes. *Nano Letters* 2005; 5(10): 2034-2038.
44. Metraux GS and Mirkin CA. Rapid thermal synthesis of silver nanoprisms with chemically tailorable thickness. *Advanced Materials* 2005; 17(4): 412-415.
45. Prokes SM, Glembocki OJ, Rendell RW, Ancona MG. Enhanced plasmon coupling in crossed dielectric/metal nanowire composite geometries and applications to surface-enhanced Raman spectroscopy. *Appl Phys Lett* 2007; 90(9): 093105.
46. Connatser RM; Prokes SM; Glembocki OJ; Schuler RL; Gardner CW; Lewis, Sr., SA; Lewis, LA. "Toward Surface Enhanced Raman Imaging of Latent Fingerprints." *Journal of Forensic Sciences*, accepted for publication August 14, 2009 to be published in the November, 2010 issue. Manuscript ID JOFS-09-292.R1.
47. De Paoli, G; Lewis, Sr., SA; Connatser, RM; Lewis, LA; Farkas, T; Schuette, EL. "Photo- And Thermal-Degradation Studies Of Select Eccrine Fingerprint Constituents." *Journal of Forensic Sciences*, accepted for publication June 27, 2009 to be published in the July, 2010 issue. Manuscript ID JOFS-09-205.R1.

VI. Dissemination of Research Findings

Presentations were made at IAI Conferences / Joint NIJ Reviews in Boston, July 2007; San Diego, July, 2008; and Tampa Bay, August, 2009.

Publications directly resulting from this work included:

R. Maggie Connatser; Sharka M. Prokes; Orest J. Glembocki; Rebecca L. Schuler; Charles W. Gardner; Samuel A. Lewis, Sr.; and Linda A. Lewis. "Toward Surface Enhanced Raman Imaging of Latent Fingerprints." *Journal of Forensic Sciences*, accepted for publication August 14, 2009 to be published in the November, 2010 issue. Manuscript ID JOFS-09-292.R1.

Giorgia De Paoli, Ph.D.1, Samuel A. Lewis, Sr., M.S.2, R. Maggie Connatser, Ph.D.2, Linda A. Lewis, Tivadar Farkas, Ph.D.3, Ellyn L. Schuette, M.S. "Photo- And Thermal-Degradation Studies Of Select Eccrine Fingerprint Constituents." *Journal of Forensic Sciences*, accepted for publication June 27, 2009 to be published in the July, 2010 issue. Manuscript ID JOFS-09-205.R1.